Heteroleptic Rare Earth Tetraalkylphospholide Cyclooctatetraenide Sandwich Complexes

Cameron N. Deakin,[1,2] Daniel J. O'Neill,[1,2] Ralph W. Adams,[2] George F. S. Whitehead,[2] and Conrad A. P. Goodwin,*[1,2]

[1] Centre for Radiochemistry Research, The University of Manchester, Oxford Road, Manchester, M13 9PL (UK).

[2] Department of Chemistry, The University of Manchester, Oxford Road, Manchester, M13 9PL (UK).

*Correspondence: conrad.goodwin@manchester.ac.uk

Abstract

A series of heteroleptic rare earth (mono)phospholide sandwich complexes of the general form [M(PC_4R_4)(COT)$(THF)_n$] (M = Sc, Y, La, Lu; R = Me, Et; COT = cyclooctatetraenide, $\{C_8H_8\}^{2-}$; *n* = 0 to 2) have been isolated by the treatment of iodide precursors, [M(COT)(I)$(THF)_n$], (**1M**, M = Sc, Y, Lu, *n* = 2; M = La, *n* = 3) with potassium phospholide salts, [K(PC_4R_4)]$_n$ (R = Me, Et). The solid-state molecular structures and speciation of these sandwich complexes depends upon both the ionic radius of the rare earth metal, along with small steric and solubility differences which arise between the two per-alkylated phospholide ligands. The smaller {PC_4Me_4} ligand gave monomeric Lewis-base free [M(C_8H_8)(PC_4Me_4)] (**2M**, M = Sc, Lu) with smaller rare earths Sc(III) and Lu(III), but moving to larger ions Y(III) and La(III), the products were poorly soluble and could only be isolated as THF-adducts, [Y(C_8H_8)(PC_4Me_4)(THF)] (**3**) and [La(C_8H_8)(PC_4Me_4)$(THF)_2$] (**4**). The slightly increased steric demands of {PC_4Et_4} gave monomeric Lewis-base free complexes for Sc(III), Lu(III), and Y(III) in [M(C_8H_8)(PC_4Et_4)] (**5M**, M = Sc, Y, Lu), whereas for La(III) a dimeric complex was isolated, [La(C_8H_8)(μ- PC_4Et_4)]$_2$ (**6**). During the course of this study, we report the synthesis and molecular structures of **1Sc** and **1Lu**, as well as [$LuI_3(THF)_3$] (**7**) for the first time. All complexes were characterised by single crystal X-ray diffraction, multi-nuclear NMR, UV-Vis-NIR and ATR-IR spectroscopies in addition to elemental analysis.

1. Introduction

Cyclopentadienide (Cp, $\{C_5H_5\}^-$) and cyclooctatetraenide (COT, $\{C_8H_8\}^{2-}$) complexes are ubiquitous in rare-earth and actinide organometallic chemistry,[1-5] and have delivered landmark advances in metal-metal bonding[6-9], molecular magnetism[9-13], and small molecule activation[14-17] (**Figure 1 A-D** for some exemple complexes). Parent Cp and substituted derivatives, Cp^R, $\{C_5R_5\}$, also find extensive use as inert spectator ligands in catalysts due to their ability to saturate coordination spheres and support additional functionality as required[18-21]. Similarly, the tuneable steric demands of substituted derivatives Cp^R (and also COT derivatives, $\{C_8R_8\}^{2-}$) using a wide range of R groups allows for greater kinetic and thermodynamic stabilisation, and control over metal redox chemistry[22-29]. Both Cp^R and $\{C_8R_8\}^{2-}$ ligand types have been used across the breadth of the periodic table to deliver isolable organometallic compounds with unique reactivities and properties[30-39].

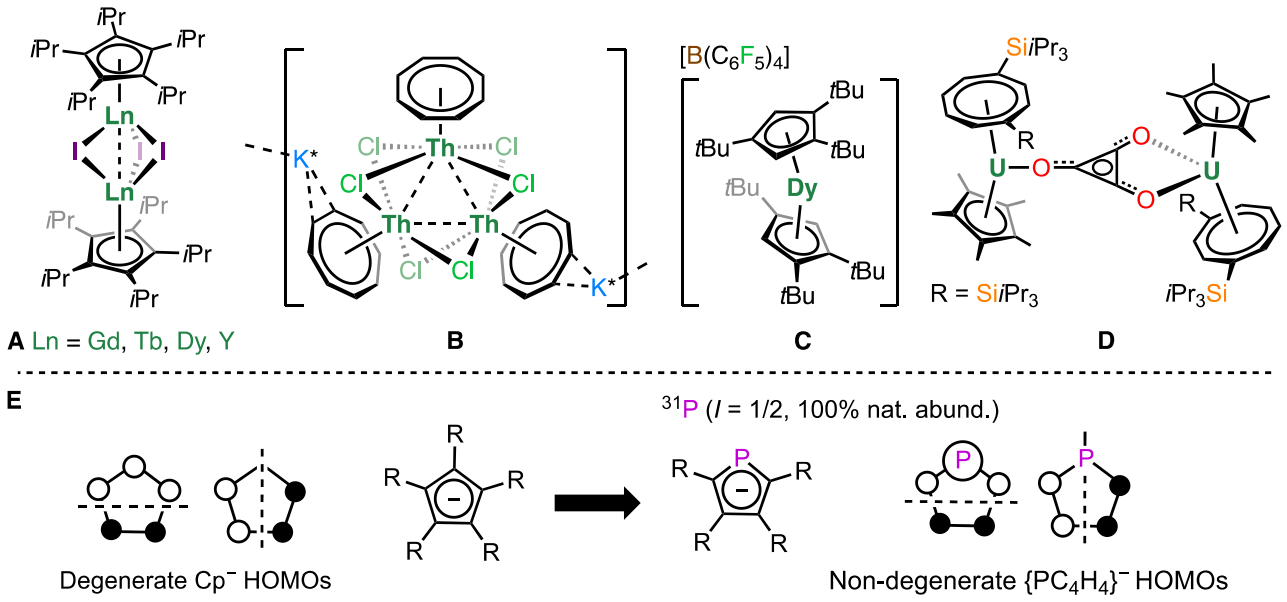

Figure 1. A-D) Examples of some landmark rare earth and actinide Cp^R and $\{C_8R_8\}^{2-}$ complexes. **E**) Schematic showing the differences in properties between $\{C_5R_5\}$ and $\{PC_4R_4\}$ anions. The e_2 HOMO level of the former is split into two non-degenerate HOMOs in the latter, one of which is concentrated somewhat on the P-atom.

Heterolide anions are analogous to the Cp anion but where one or more of the ring C-atoms has been replaced with a heteroatom (*i.e.* $\{C_{5-n}R_{5-n}E_n\}$ where E is a heteroatom), such as phosphorus[40,41]. The chemistry of rare earth and actinide complexes supported by (mono)phospholide ligands, $\{PC_4R_4\}$, remains poorly developed with only 80 such structurally characterised examples in the CCDC by June 2024[42], the vast majority of which has been undertaken by Nief, Mathey, Le Floch, and co-workers who contributed seminal results in the research area[42-51]. The chemistry of $\{PC_4R_4\}$ ligands complements, but is divergent from, that of their Cp counterparts (**Figure 1 E**)[52]. For example, the heteroatom alters the donor and vibrational properties with implications for molecular magnetism such as with $[Dy(Dtp)_2]^+$ (Dtp = $\{PC_4$-2,5-*t*Bu_2-3,4-$Me_2\}$)[53] and [Er(COT)(Dsp)] (Dsp = $\{PC_4$-2,5-TMS_2-3,4-$Me_2\}$; TMS = $SiMe_3$)[54]. Similarly, the electronic differences between Cp^R and $\{PC_4R_4\}$ can significantly alter the redox properties of metal complexes.[29,55,56]

Due to the barrier to entry in phospholide chemistry whereby ligand syntheses can be capricious and require multiple steps of air-free synthesis, much of the basic coordination chemistry such as their steric demands *versus* similarly substituted Cp^R ligands[57], and the influence of oligomerisation on their crystallisation properties remains poorly defined. Herein we report the synthesis of heteroleptic COT phospholide complexes [M(COT)(TMP)] (**2M**, M = Sc, Lu), [Y(COT)(TMP)(THF)] (**3**), [La(COT)(TMP)$(THF)_2$] (**4**), [M(COT)(TEP)] (**5M**, M = Sc, Y, Lu), and dimeric [La(COT)(μ-TEP)]$_2$ (**6**) by salt elimination between rare earth COT iodide complexes [M(COT)(I)$(THF)_n$] (**1M**, M = Sc, Y, Lu, n = 2; M = La, n = 3) and potassium salts of the alkylated phospholide ligands TMP (TMP = $\{PC_4Me_4\}$) and TEP (TEP = $\{PC_4Et_4\}$). All complexes were characterised by single crystal X-ray diffraction (SCXRD), multi-nuclear NMR (^{1}H, ^{13}C, ^{31}P, ^{45}Sc, ^{89}Y, as appropriate), UV-Vis-NIR and ATR-IR spectroscopies, and elemental analysis.

2. Experimental

2.1. General Methods

Unless otherwise described, all syntheses and manipulations were conducted under BOC PureShield argon (99.995%) with rigorous exclusion of oxygen and water using Schlenk line and glove box techniques in an MBraun Lab Star™. 3 Å molecular sieves were activated by heating for 8 hours at 300°C, 10^{-3} mbar. THF, *n*-hexane, and toluene were degassed by sparging and dried by passage through neutral alumina columns (INERT Corp.). THF was then degassed under vacuum and stored over 3 Å molecular sieves for 7 days before use. *n*-hexane and toluene were degassed under vacuum and stored over a K mirror and used immediately. C_6D_6 and C_4D_8O (Merck) were dried by refluxing over K metal, or CaH_2 in the case of C_5D_5N (Merck), for 4-5 days followed by vacuum transfer and storage in a J. Youngs valve appended vessel. $[MI_3(THF)_3]$ (M = Sc, Lu) were prepared from metal powder (*ca*. 200 mesh) in analogy to other rare earth triiodide precursors[58]. KTMP, KTEP and $[La(COT)(I)(THF)_3]$ were prepared as described previously[59-61]. Cyclooctatetraene (C_8H_8) was degassed and stored over 3 Å molecular sieves for 7 days prior to use, and K_2COT was prepared as an off-white powder by combining C_8H_8 with a slight excess of freshly cleaned K-metal in THF at room temperature for 18 hours, followed by filtration and removal of the volatiles under vacuum[62]. Glass-fiber filter discs and PTFE-coated stirrer bars were stored in an oven (150°C) for at least 12 hours before use, and glassware was dried *under vacuum* (10^{-3} mbar) after strong heating with a butane flame. Solution phase UV-Vis-NIR spectra were collected at ambient temperature using a PerkinElmer Lambda 1050 UV-Vis-NIR spectrometer. Solutions were contained in a low volume (1 mL) screw-capped quartz cuvette with a 1 cm path length. ATR FT-IR spectra of microcrystalline samples were collected using a Bruker ALPHA II FT-IR spectrometer equipped with a Platinum ATR module with a diamond window. NMR spectroscopic data collection was performed on a Bruker Avance III

(400 MHz) or a Bruker Advance III HD (400 MHz). Elemental microanalyses (C/H/N) were carried out by Martin Jennings and Anne Davies at the University of Manchester.

2.2. Synthesis

[Sc(COT)(I)(THF)$_2$] (**1Sc**). THF (30 mL) was added to a pre-cooled (–98°C) glass Schlenk vessel, equipped with a PTFE-coated stirrer bar, containing solid [ScI$_3$(THF)$_3$] (2.568 g, 4 mmol). Separately, THF (15 mL) was added to a glass Schlenk vessel, equipped with a PTFE-coated stirrer bar, containing solid K$_2$COT (0.729 g, 4 mmol) which immediately formed a dark orange solution which was then added dropwise to the [ScI$_3$(THF)$_3$] solution. The mixture was allowed to warm to room temperature and quickly became orange with a fine white precipitate, presumed to be KI. After stirring at room temperature overnight (16 hours), the solids were allowed to settle before filtration through a glass microfibre filter disc. Concentration of the clear orange supernatant to ca. 10 mL gave a large quantity of orange solids which were heated into solution and allowed to cool slowly to give large orange blocks of **1Sc**. This mixture was stored at 5°C for 2 hours followed by –30°C for 16 hours to increase the yield. Crystals were isolated by decanting the supernatant followed by drying under vacuum (10^{-3} mbar, 2 hours). A second crop was obtained in a similar fashion (combined yield = 1.363 g, 81.1%).

Elemental analysis on $C_{16}H_{24}O_2ISc$ calc. (%): C = 45.73, H = 5.76, N = 0.00; found (%): C = 42.36, H = 5.40, N = 0.00.

^{1}H NMR (C_6D_6 and C_5D_5N 400.13 MHz, 298 K): δ = 6.72 (s, 8H, COT C*H*), 3.49 (m, 8H, THF *H*), 1.41 (m, 8H, THF *H*).

^{13}C{^{1}H} NMR (C_6D_6 and C_5D_5N, 100.62 MHz, 298 K): δ = 97.90 (s, COT *C*), 67.44 (s, THF *C*), 25.42 (s, THF *C*).

UV-vis-NIR (THF): λ_{max} (cm^{-1}; ε) = A broad feature extends from ~400 nm (20,000 cm^{-1}) into the UV region, and beyond our spectral range.

FT-IR (ATR, microcrystalline) cm^{-1} = 3,027 (vw), 2,970 (m), 2,951 (w), 2,892 (w), 1,874 (vw), 1,766 (vw), 1,637 (vw), 1,469 (w), 1,447 (w), 1,361 (vw), 1,342 (w), 1,313 (w), 1,295 (vw), 1,243 (w), 1,213 (vw), 1,174 (vw), 1,065 (vw), 1,036 (w), 1,011 (vs), 956 (vw), 927 (w), 906 (vs), 855 (vs), 787 (m), 775 (m), 758 (m), 715 (vs), 666 (vs), 617 (s), 600 (s), 575 (s), 567 (s), 559 (s), 551 (s), 530 (vs), 504 (s), 493 (s), 475 (m), 462 (s), 452 (m), 427 (m), 419 (m), 409 (m).

[Lu(COT)(I)$(THF)_2$] (**1Lu**). The complex was prepared analogously to **1Sc** above – [$LuI_3(THF)_3$] (3.088 g, 4 mmol), K_2COT (0.729 g, 4 mmol). The dark brown solution gave **1Lu** as colourless blocks over two crystalline crops (combined yield = 1.275 g, 58%).

Elemental analysis on $C_{16}H_{24}O_2ILu$ calc. (%): C = 34.92, H = 4.40, N = 0.00; found (%): C = 33.94, H = 4.27, N = 0.00.

^{1}H NMR (C_6D_6 and C_5D_5N, 400.13 MHz, 298 K): δ = 6.63 (s, 8H, COT C*H*), 3.54 (m, 8H, THF-*H*), 1.43 (m, 8H, THF *H*).

$^{13}C\{^1H\}$ NMR (C_6D_6 and C_5D_5N, 100.62 MHz, 298 K): 94.52 (s, COT *C*), 67.81 (s, THF *C*), 25.79 (s, THF *C*).

UV-vis-NIR (THF): λ_{max} (cm^{-1}; ε) = A broad feature extends from ~350 nm (28,000 cm^{-1}) into the UV region, and beyond our spectral range.

FT-IR (ATR, microcrystalline) cm^{-1} = 3,019 (w), 2,970 (s), 2,955 (s), 2,927 (m), 2,894 (s), 1,870 (vw), 1,850 (vw), 1,745 (vw), 1,613 (vw), 1,482 (w), 1,469 (m), 1,445 (s), 1,344 (m), 1,311 (m), 1,297 (vw), 1,245 (w), 1,233 (vw), 1,182 (vw), 1,137 (vw), 1,093 (vw), 1,067 (vw), 1,007 (vs), 956 (vw), 927 (s), 917 (s), 900 (vs), 857 (vs), 775 (vs), 752 (s), 715 (vs), 668 (vs), 573 (s), 543 (s), 534 (m), 520 (s), 504 (m), 489 (m), 483 (m), 477 (w), 462 (m), 454 (m), 446 (w), 440 (w), 423 (w), 409 (w).

[Y(COT)(I)(THF)$_2$] (**1Y**). THF (40 mL) was added to a glass Rotaflo®-valve appended vessel, equipped with a PTFE-coated stirrer bar, containing Y^0 metal filings (0.391 g, 4.4 mmol). The colourless suspension was cooled to (–98°C) and cyclooctatetraene (0.5 mL, 4.4 mmol) was added *via* a glass syringe followed by the dropwise addition of a THF solution of I_2 (15 mL). The mixture was allowed to warm to room temperature and quickly became opaque orange and then heated to 50 °C for 72 hours over which time the mixture turned light yellow with some fine grey solids. The solids were then allowed to settle before filtration at 50°C through a glass microfibre filter disc. Concentration of the clear orange supernatant to ca. 10 mL gave a large quantity of orange solids which were heated into solution and allowed to cool slowly to give large orange blocks of **2Y**. This mixture was stored at 5°C for 2 hours followed by –30°C for 16 hours to increase the yield. Crystals were isolated by decanting the supernatant followed by drying under vacuum (10^{-3} mbar, 2 hours). A second crop was obtained in a similar fashion (combined yield = 1.009 g, 49.4%).

Elemental analysis on $C_{16}H_{24}O_2IY$ calc. (%): C = 41.40, H = 5.21, N = 0.00; found (%): C = 40.35, H = 5.14, N = 0.00.

^{1}H NMR (C_6D_6 and C_5D_5N, 400.13 MHz, 298 K): δ = 6.69 (s, 8H, COT C*H*), 3.55 (m, 8H, THF *H*), 1.43 (m, 8H, THF *H*).

^{13}C{^{1}H} NMR (C_6D_6 and C_5D_5N, 100.62 MHz, 298 K): 94.52 (s, COT *C*), 67.81 (s, THF *C*), 25.79 (s, THF *C*).

UV-vis-NIR (THF): λ_{max} (cm^{-1}; ε) = A broad feature extends from ~400 nm (24,000 cm^{-1}) into the UV region, and beyond our spectral range.

FT-IR (ATR, microcrystalline) cm^{-1} = 405 (m) 413 (w) 419 (w) 432 (w) 446 (w) 464 (m) 479 (w) 489 (m) 504 (s) 516 (m) 532 (m) 538 (m) 551 (m) 575 (vs) 602 (s) 668 (vs) 711 (vs) 750 (s) 775 (s) 857 (vs) 896 (vs) 915 (s) 1009 (vs) 1096 (vw) 1176 (vw) 1245 (w) 1260 (vw) 1309 (w) 1344 (s) 1445 (w) 1469 (vw) 1482 (s) 1556 (m) 1615 (s) 1747 (vw) 1852 (vw) 2892 (vw) 2955 (vw) 2970 (vw) 3015 (vw).

[Sc(COT)(TMP)] (**2Sc**). THF (15 mL) was added to a pre-cooled (–98°C) stirring mixture of solid [Sc(COT)(I)(THF)$_2$] (**1Sc**) (0.420 g, 1 mmol) and KTMP (0.178 g, 1 mmol) in a glass Schlenk vessel equipped with a PTFE-coated stirrer bar. The mixture was allowed to warm to room temperature and quickly became light-yellow with a fine white precipitate, presumed to be KI. After stirring at room temperature overnight (16 hours), the volatiles were removed under vacuum (10^{-3} mbar) which left a light-yellow powder. Toluene (20 mL) was added and briefly (< 1 min) refluxed with manual agitation to loosen solids from the vessel walls. The light-yellow solution and fine white solids were allowed to settle before filtration through a glass microfibre filter disc. Concentration of the bright yellow supernatant to ca. 3 mL gave a large quantity of colourless solids which were heated into solution and allowed to cool slowly to room temperature, stored at 5°C for 2 hours followed by –30°C for 16 hours to give large colourless blocks of **2Sc**. A second crop was obtained in a similar fashion (combined yield = 0.150 g, 52%).

Elemental analysis on $C_{16}H_{20}PSc$ calc. (%): C = 66.66, H = 6.99, N = 0.00; found (%): C = 66.81, H = 7.10, N = 0.00.

^{1}H NMR (C_6D_6, 400.13 MHz, 298 K): δ = 6.31 (s, 8H, COT C*H*), 1.90 (d, $^3J_{HP}$ = 10.0 Hz, 6H, TMP 2,5-(C*H*$_3$)$_2$), 1.67 (s, 6H, TMP 3,4-(C*H*$_3$)$_2$).

^{13}C{^{1}H} NMR (C_6D_6, 100.62 MHz, 298 K): δ = 140.20 (d, J_{CP} = 51.8 Hz, TMP 2,5-*C*(CH$_3$)$_2$), 131.56 (d, J_{CP} = 4.4 Hz, TMP 3,4-*C*(CH$_3$)$_2$), 95.78 (s, COT *C*), 15.72 (d, J_{CP} = 26.8 Hz, TMP 2,5-C(*C*H$_3$)$_2$), 13.79 (s, TMP 3,4-C(*C*H$_3$)$_2$).

^{31}P{^{1}H} NMR (C_6D_6, 161.95 MHz, 298 K): δ = 95.67 (s, TMP *P*).

^{45}Sc NMR (C_6D_6, 97.15 MHz, 298 K): δ = 13.04 (s).

UV-vis-NIR (THF): λ_{max} (cm^{-1}; ε) = A broad feature extends from ~400 nm (24,000 cm^{-1}) into the UV region, and beyond our spectral range.

FT-IR (ATR, microcrystalline) cm^{-1} = 3,044 (vw), 2,994 (vw), 2,943 (m), 2,908 (s), 2,855 (s), 2,742 (vw), 2,721 (vw), 1,862 (w), 1,759 (m), 1,620 (vw), 1,492 (w), 1,469 (vw), 1,447 (s), 1,430 (m), 1,375 (vs), 1,313 (m), 1,260 (w), 1,093 (w), 1,015 (m), 898 (vs), 804 (vw), 773 (s), 754 (vs), 709 (vs), 569 (m), 553 (w), 522 (s), 495 (m), 483 (s), 464 (w).

[Lu(COT)(TMP)] (**2Lu**). The complex was prepared analogously to **2Sc** above – [Lu(COT)(I)$(THF)_2$] (0.550 g, 1 mmol), KTEP (0.178 g, 1 mmol). The light-yellow solution gave **2Lu** as colourless blocks over two crystalline crops (combined yield = 0.161 g, 38%). Elemental analysis on $C_{16}H_{20}PLu$ calc. (%): C = 45.94, H = 4.82, N = 0.00; found (%): C = 45.84, H = 4.80, N = 0.00.

^{1}H NMR (C_6D_6, 400.13 MHz, 298 K): δ = 6.24 (s, 8H, COT C*H*), 1.96 (d, $^{3}J_{HP}$ = 9.9 Hz, 6H, TMP 3,4-(C*H*$_3$)$_2$), 1.76 (s, 6H, TMP 2,5-(C*H*$_3$)$_2$).

$^{13}C\{^{1}H\}$ NMR (C_6D_6, 100.62 MHz, 298 K): δ = 141.68 (d, J_{CP} = 51.5 Hz, TMP 2,5-*C*$(CH_3)_2$), 132.79 (d, J_{CP} = 4.2 Hz, TMP 3,4-*C*$(CH_3)_2$), 93.50 (s, COT *C*), 15.01 (d, J_{CP} = 26.4 Hz, TMP 2,5-C(*C*$H_3)_2$), 13.50 (s, TMP 3,4-C(*C*$H_3)_2$).

$^{31}P\{^{1}H\}$ NMR (C_6D_6, 161.95 MHz, 298 K): δ = 88.36 (s, TEP *P*).

UV-vis-NIR (THF): λ_{max} (cm^{-1}; ε) = A broad feature extends from ~380 nm (26,000 cm^{-1}) into the UV region, and beyond our spectral range.

FT-IR (ATR, microcrystalline) cm^{-1} = 3,040 (vw), 2,980 (vw), 2,908 (s), 2,853 (m), 2,756 (vw), 2,738 (vw), 2,721 (vw), 2,692 (vw), 1,852 (vw), 1,747 (w), 1,603 (vw), 1,478 (w), 1,443 (m), 1,426 (m), 1,375 (vs), 1,305 (w), 1,260 (w), 1,217 (vw), 1,167 (vw), 1,147 (w), 1,095 (m), 1,054 (w), 1,013 (m), 954 (w), 892 (vs), 834 (w), 802 (m), 767 (m), 748 (s), 705 (vs), 625 (vs), 608 (s), 602 (s), 580 (s), 559 (m), 524 (vs), 481 (vs), 464 (s), 438 (s), 419 (s).

[Y(COT)(TMP)(THF)] (**3**). The complex was prepared analogously to **2Sc** above – [Y(COT)(I)(THF)$_2$] (0.464 g, 1 mmol), KTEP (0.178 g, 1 mmol). The light-yellow solution gave **3** as colourless blocks over a single crystalline crop from THF (yield = 0.075 g, 19%).

Elemental analysis on $C_{20}H_{28}OPY$ for 1 THF calc. (%): C = 59.41, H = 6.98, N = 0.00; for 0 THF calc. (%): C = 57.84, H = 6.07, N = 0.00; found (%): C = 57.72, H = 6.12, N = 0.00.

^{1}H NMR (C_6D_6 and C_4D_8O, 400.13 MHz, 298 K): δ = 6.14 (d, J_{HY} = 1.0 Hz, 8H, COT C*H*), 3.53 (s, THF *H*), 1.94 (d, $^3J_{HP}$ = 10.1 Hz, 6H, TMP 2,5-(C*H*$_3$)$_2$), 1.90 (s, 6H, TMP 3,4-(C*H*$_3$)$_2$), 1.42 (s, THF *H*).

^{13}C{^{1}H} NMR (C_6D_6 and C_4D_8O, 100.62 MHz, 298 K): δ = 141.14 (d, J_{CP} = 45.4 Hz, TMP 2,5-*C*(CH$_3$)$_2$), 132.44 (d, J_{CP} = 3.2 Hz, TMP 3,4-*C*(CH$_3$)$_2$), 98.15 (s, COT *C*), 15.62 (d, J_{CP} = 26.4 Hz, TMP 2,5-C(*C*H$_3$)$_2$), 14.01 (s, TMP 3,4-C(*C*H$_3$)$_2$).

^{31}P{^{1}H} NMR (C_6D_6 and C_4D_8O, 161.95 MHz, 298 K): δ = 84.78 (d, J_{PY} = 9.0 Hz, TMP *P*).

^{89}Y-^{1}H HSQC NMR (C_6D_6 and C_4D_8O, 19.60 MHz / 399.92 MHz, 298 K): δ = –155.43 / 5.60 (*Y*-COT-*H*).

UV-vis-NIR (THF): λ_{max} (cm^{-1}; ε) = A broad feature extends from ~400 nm (24,000 cm^{-1}) into the UV region, and beyond our spectral range.

FT-IR (ATR, microcrystalline) cm^{-1} = 3,043 (vw), 3,009 (vw), 2,955 (vw), 2,935 (w), 2,925 (w), 2,904 (w), 2,869 (w), 2,855 (w), 2,723 (vw), 1,846 (vw), 1,745 (vw), 1,599 (vw), 1,545 (vw), 1,469 (w), 1,449 (s), 1,424 (w), 1,377 (vs), 1,320 (vw), 1,261 (vw), 1,178 (vw), 1,147 (m), 1,097 (vw), 1,026 (w), 1,009 (m), 956 (w), 906 (vs), 892 (vs), 839 (m), 781 (m), 762 (w), 713 (vs), 625 (s), 606 (s), 592 (s), 578 (m), 567 (m), 557 (s), 549 (s), 538 (m), 530 (s), 510 (vs), 483 (vs), 464 (s), 454 (s), 442 (m), 430 (s), 417 (m), 407 (vs).

[La(COT)(TMP)(THF)$_2$] (**4**). The complex was prepared analogously to **2Sc** above – [La(COT)(I)(THF)$_3$] (0.568 g, 1 mmol),[63] KTEP (0.178 g, 1 mmol). The light-yellow solution gave **4** as colourless blocks over a single crystalline crop from THF (yield = 0.320 g, 61%).

Elemental analysis on $C_{24}H_{36}O_2PLa$ calc. (%): C = 54.76, H = 6.89, N = 0.00; found (%): C = 54.46, H = 6.94, N = 0.00.

^{1}H NMR (C_6D_6 and C_5D_5N, 400.13 MHz, 298 K): δ = 6.25 (s, 8H, COT C*H*), 3.51 (m, 8H, THF *H*), 2.09 (s, 6H, TMP 3,4-(C*H*$_3$)$_2$), 1.76 (d, $^3J_{HP}$ = 9.7 Hz, 6H, TMP 2,5-(C*H*$_3$)$_2$), 1.43 (m, 8H, THF *H*).

^{13}C{^{1}H} NMR (C_6D_6 and C_5D_5N, 100.62 MHz, 298 K): δ = 140.91 (d, J_{CP} = 43.3 Hz, TMP 2,5-*C*(CH$_3$)$_2$), 135.95 (d, J_{CP} = 2.7 Hz, TMP 3,4-*C*(CH$_3$)$_2$), 93.20 (s, COT *C*), 67.7 (s, THF), 25.74 (s, THF), 15.51 (d, J_{CP} = 26.3 Hz, TMP 2,5-C(*C*H$_3$)$_2$), 13.50 (s, TMP 3,4-C(*C*H$_3$)$_2$).

^{31}P{^{1}H} NMR (C_6D_6 and C_5D_5N, 161.95 MHz, 298 K): δ = 94.61 (TMP *P*).

UV-vis-NIR (THF): λ_{max} (cm^{-1}; ε) = A broad feature extends from ~400 nm (24,000 cm^{-1}) into the UV region, and beyond our spectral range.

FT-IR (ATR, microcrystalline) cm^{-1} = 417 (m), 425 (m), 442 (m), 452 (m), 460 (m), 475 (s), 491 (m), 514 (s), 536 (m), 578 (s), 612 (s), 666 (vs), 697 (vs), 748 (m), 765 (w), 832 (vs), 865 (vs), 882 (vs), 894 (s), 904 (s), 915 (m), 927 (w), 956 (vw), 1,021 (vs), 1,034 (vs), 1,139 (w), 1,171 (w), 1,245 (vw), 1,293 (vw), 1,305 (vw), 1,336 (w), 1,361 (vw), 1,375 (w), 1,402 (w), 1,447 (s), 1,488 (vw), 2,713 (vw), 2,746 (vw), 2,853 (s), 2,879 (s), 2,904 (s), 2,923 (w), 2,949 (m), 2,959 (w), 3,021 (w), 1,719 (vw), 1,580 (vw), 1,825 (vw), 1,092 (vw).

[Sc(COT)(TEP)] (**5Sc**). THF (15 mL) was added to a pre-cooled (–98°C) stirring mixture of solid [Sc(COT)(I)(THF)$_2$] (**1Sc**) (0.420 g, 1 mmol) and KTEP (0.234 g, 1 mmol) in a glass Schlenk vessel equipped with a PTFE-coated stirrer bar. The mixture was allowed to warm to room temperature and quickly became light-yellow with a fine white precipitate, presumed to be KI. After stirring at room temperature overnight (16 hours), the volatiles were removed under vacuum (10^{-3} mbar) which left a light-yellow powder. Toluene (20 mL) was added and briefly (< 1 min) refluxed with manual agitation to loosen solids from the vessel walls. The light-yellow solution and fine white solids were allowed to settle before filtration through a

glass microfibre filter disc. Concentration of the bright yellow supernatant to ca. 2 mL gave a large quantity of colourless solids which were heated into solution and allowed to cool slowly to room temperature, stored at 5°C for 2 hours followed by –30°C for 16 hours to give large colourless blocks of **5Sc**. Concentration of the supernatant to ca. 1 mL did not afford any further crops (yield = 0.176 g, 51%).

Elemental analysis on $C_{20}H_{28}PSc$ calc. (%): C = 69.75, H = 8.20, N = 0.00; found (%): C = 69.20, H = 8.09, N = 0.00.

^{1}H NMR (C_6D_6, 400.13 MHz, 298 K): δ = 6.30 (s, 8H, COT C*H*), 2.24 (m, 8H, TEP (C*H*$_2$)$_4$), 1.21 (t, $^{3}J_{HH}$ = 7.5 Hz, 6H, TEP 2,5-(C*H*$_3$)$_2$), 0.83 (t, $^{3}J_{HH}$ = 7.5 Hz, 6H, TEP 3,4-(C*H*$_3$)$_2$).

^{13}C{^{1}H} NMR (C_6D_6, 100.62 MHz, 298 K): δ = 149.70 (d, J_{CP} = 53.6 Hz, TEP 2,5-*C*(CH$_2$CH$_3$)$_2$), 136.55 (d, J_{CP} = 5.0 Hz, TEP 3,4-*C*(CH$_2$CH$_3$)$_2$), 95.53 (s, COT *C*), 23.88 (d, J_{CP} = 20.6 Hz, TEP 2,5-(*C*H$_2$CH$_3$)$_2$), 21.73 (s, TEP 2,5-(CH$_2$*C*H$_3$)$_2$), 17.22 (d, J_{CP} = 13.0 Hz, TEP 3,4-(*C*H$_2$CH$_3$)$_2$), 15.93 (s, TEP 3,4-(CH$_2$*C*H$_3$)$_2$).

^{31}P{^{1}H} NMR (C_6D_6, 161.95 MHz, 298 K): δ = 88.49 (s, TEP *P*).

^{45}Sc NMR (C_6D_6, 97.15 MHz, 298 K): δ = −18.15 (s).

UV-vis-NIR (THF): λ_{max} (cm^{-1}; ε) = A broad feature extends from ~400 nm (24,000 cm^{-1}) into the UV region, and beyond our spectral range.

FT-IR (ATR, microcrystalline) cm^{-1} = 2,959 (vs), 2,927 (s), 2,869 (s), 1,864 (vw), 1,761 (w), 1,622 (vw), 1,492 (vw), 1,469 (m), 1,451 (s), 1,432 (m), 1,404 (vw), 1,389 (vw), 1,371 (s), 1,311 (m), 1,264 (w), 1,149 (vw), 1,112 (w), 1,100 (w), 1,089 (m), 1,054 (s), 1,007 (vw), 974 (vw), 962 (vw), 898 (vs), 843 (vw), 814 (w), 781 (s), 754 (vs), 711 (vs), 631 (m), 617 (w), 600 (w), 573 (s), 555 (w), 536 (m), 524 (m), 491 (s), 462 (m), 440 (vs), 419 (vs).

[Y(COT)(TEP)] (**5Y**). The complex was prepared analogously to **5Sc** above – [Y(COT)(I)(THF)$_2$] (0.464 g, 1 mmol), KTEP (0.235 g, 1 mmol). The light-yellow solution gave **5Y** as colourless blocks over a single crystalline crop (yield = 0.212 g, 55%).

Elemental analysis on $C_{20}H_{28}PY$ calc. (%): C = 61.86, H = 7.27, N = 0.00; found (%): C = 61.13, H = 6.96, N = 0.00.

^{1}H NMR (C_6D_6 and C_5D_5N, 400.13 MHz, 298 K): δ = 6.14 (s, 8H, COT C*H*), 2.48 (q, $^{3}J_{HH}$ = 7.5 Hz, 4H, TEP 2,5-(C*H*$_3$)$_2$), 2.18 (m, 4H, TEP 3,4-(C*H*$_3$)$_2$), 1.11 (t, $^{3}J_{HH}$ = 7.4 Hz, 6H, TEP 2,5-(C*H*$_3$)$_2$), 1.04 (t, $^{3}J_{HH}$ = 7.5 Hz, 6H, TEP 3,4-(C*H*$_3$)$_2$).

$^{13}C\{^{1}H\}$ NMR (C_6D_6 and C_5D_5N, 100.62 MHz, 298 K): δ = 150.54 (dd, J_{CP} = 48.4 Hz, J_{CY} = 1.0 Hz, TEP 2,5-*C*(CH$_2$CH$_3$)$_2$), 137.63 (d, J_{CP} = 4.0 Hz, TEP 3,4-*C*(CH$_2$CH$_3$)$_2$), 93.90 (d, J_{CY} = 2.6 Hz, COT *C*), 24.13 (d, J_{CP} = 21.1 Hz, TEP 2,5-(*C*H$_2$CH$_3$)$_2$), 21.93 (s, TEP 2,5-(CH$_2$*C*H$_3$)$_2$), 18.19 (d, J_{CP} = 11.7 Hz, TEP 3,4-(*C*H$_2$CH$_3$)$_2$), 16.29 (s, TEP 3,4-(CH$_2$*C*H$_3$)$_2$).

$^{31}P\{^{1}H\}$ NMR (C_6D_6 and C_5D_5N, 161.95 MHz, 298 K): δ = 82.28 (m, TEP *P*).

^{89}Y-^{1}H HSQC NMR (C_6D_6 and C_5D_5N, 19.60 MHz / 399.92 MHz, 298 K): δ = –91.39 / 6.29 (*Y*-COT-*H*).

UV-vis-NIR (THF): λ_{max} (cm^{-1}; ε) = A broad feature extends from ~400 nm (24,000 cm^{-1}) into the UV region, and beyond our spectral range.

FT-IR (ATR, microcrystalline) cm^{-1} = 3,033 (vs), 2,962 (vw), 2,925 (vw), 2,867 (w), 1,867 (vs), 1,753 (vs), 1,611 (vs), 1,465 (m), 1,451 (vw), 1,432 (m), 1,398 (s), 1,371 (vw), 1,311 (w), 1,262 (s), 1,229 (vs), 1,149 (s), 1,097 (m), 1,087 (m), 1,054 (vw), 1,019 (s), 1,013 (s), 1,005 (s), 958 (vs), 892 (vw), 839 (s), 812 (s), 771 (s), 746 (vw), 705 (vw), 629 (w), 617 (w), 606 (w), 580 (m), 567 (w), 547 (m), 530 (w), 508 (m), 485 (w), 475 (w), 462 (m), 432 (vw), 415 (vw).

[Lu(COT)(TEP)] (**5Lu**). The complex was prepared analogously to **5Sc** above – [Lu(COT)(I)(THF)$_2$] (0.550 g, 1 mmol), KTEP (0.235 g, 1 mmol). The light-yellow solution gave **5Lu** as colourless blocks over a single crystalline crop (yield = 0.277 g, 58%).

Elemental analysis on $C_{20}H_{28}PLu$ calc. (%): C = 50.64, H = 5.95, N = 0.00; found (%): C = 50.89, H = 5.77, N = 0.00.

^{1}H NMR (C_6D_6, 400.13 MHz, 298 K): δ = 6.24 (s, 8H, COT C*H*), 2.34 (dq, $^{3}J_{HP}$ = 8.8 Hz, $^{3}J_{HH}$ = 7.5 Hz, 4H, TEP 2,5-(C*H*$_3$)$_2$), 2.19 (q, $^{3}J_{HH}$ = 7.6 Hz, 4H, TEP 3,4-(C*H*$_3$)$_2$), 1.19 (t, $^{3}J_{HH}$ = 7.5 Hz, 6H, TEP 2,5-(C*H*$_3$)$_2$), 0.85 (t, $^{3}J_{HH}$ = 7.5 Hz, 6H, TEP 3,4-(C*H*$_3$)$_2$).

^{13}C{^{1}H} NMR (C_6D_6, 100.62 MHz, 298 K): δ = 151.43 (d, J_{CP} = 53.6 Hz, TEP 2,5-*C*(CH$_2$CH$_3$)$_2$), 136.55 (d, J_{CP} = 5.0 Hz, TEP 3,4-*C*(CH$_2$CH$_3$)$_2$), 95.53 (s, COT *C*), 23.88 (d, J_{CP} = 20.6 Hz, TEP 2,5-(*C*H$_2$CH$_3$)$_2$), 21.73 (s, TEP 2,5-(CH$_2$*C*H$_3$)$_2$), 17.22 (d, J_{CP} = 13.0 Hz, TEP 3,4-(*C*H$_2$CH$_3$)$_2$), 15.82 (s, TEP 3,4-(CH$_2$*C*H$_3$)$_2$).

^{31}P{^{1}H} NMR (C_6D_6, 161.95 MHz, 298 K): δ = 81.36 (s, TEP *P*).

UV-vis-NIR (THF): λ_{max} (cm^{-1}; ε) = A broad feature extends from ~380 nm (26,000 cm^{-1}) into the UV region, and beyond our spectral range.

FT-IR (ATR, microcrystalline) cm^{-1} = 2,959 (vs), 2,925 (s), 2,867 (s), 2,842 (w), 2,803 (vw), 1,856 (vw), 1,751 (w), 1,613 (vw), 1,467 (m), 1,449 (vs), 1,432 (m), 1,398 (vw), 1,371 (vs), 1,311 (m), 1,262 (w), 1,149 (vw), 1,097 (w), 1,085 (w), 1,071 (vw), 1,054 (s), 1,003 (vw), 960 (vw), 892 (vs), 839 (vw), 812 (vw), 771 (w), 748 (s), 707 (vs), 619 (m), 612 (m), 567 (s), 543 (w), 528 (m), 510 (w), 489 (s), 464 (m), 446(m), 434 (vs), 419 (s), 411 (s).

[La(COT)(μ-TEP)]$_2$ (**6**). The complex was prepared analogously to **5Sc** above – [La(COT)(I)(THF)$_3$] (0.293 g, 0.5 mmol),[63] KTEP (0.117 g, 0.5 mmol). The light-yellow solution gave **6** as light-yellow blocks over a single crystalline crop and a single crop (yield = 0.0248 g, 6%).

Elemental analysis on $C_{40}H_{56}P_2La_2$ calc. (%): C = 54.80, H = 6.44, N = 0.00; found (%): C = 52.56, H = 6.44, N = 0.00.

^{1}H NMR (C_6D_6 and C_5D_5N, 400.13 MHz, 298 K): δ = 6.31 (s, 8H, COT C*H*), 2.63 (dq, $^{3}J_{HP}$ = 15.1 Hz, $^{3}J_{HH}$ = 7.4 Hz, 4H, TEP 2,5-(C*H*$_3$)$_2$), 2.44 (m, 2H, TEP 3,4-(C*H*$_3$)), 2.20 (m, 2H, TEP 3,4-(C*H*$_3$)), 1.16 (t, $^{3}J_{HH}$ = 7.4 Hz, 6H, TEP 2,5-(C*H*$_3$)$_2$), 1.11 (t, $^{3}J_{HH}$ = 7.5 Hz, 6H, TEP 3,4-(C*H*$_3$)$_2$).

$^{13}C\{^{1}H\}$ NMR (C_6D_6 and C_5D_5N, 100.62 MHz, 298 K): δ = 151.58 (d, J_{CP} = 45.0 Hz, TEP 2,5-$\underline{C}(CH_2CH_3)_2$), 136.55 (d, J_{CP} = 5.0 Hz, TEP 3,4-$\underline{C}(CH_2CH_3)_2$), 95.53 (s, COT $\underline{C}$), 23.88 (d, J_{CP} = 20.6 Hz, TEP 2,5-($\underline{C}H_2CH_3)_2$), 21.73 (s, TEP 2,5-($CH_2\underline{C}H_3)_2$), 17.22 (d, J_{CP} = 13.0 Hz, TEP 3,4-($\underline{C}H_2CH_3)_2$), 15.93 (s, TEP 3,4-($CH_2\underline{C}H_3)_2$).

$^{31}P\{^{1}H\}$ NMR (C_6D_6 and C_5D_5N, 161.95 MHz, 298 K): δ = 93.69 (s, TEP $\underline{P}$).

UV-vis-NIR (THF): λ_{max} (cm^{-1}; ε) = A broad feature extends from ~500 nm (20,000 cm^{-1}) into the UV region, and beyond our spectral range. FT-IR (ATR, microcrystalline) cm^{-1} = 3,036 (s), 3,007 (s), 2,957 (vw), 2,925 (vw), 2,865 (w), 2,781 (m), 2,738 (s), 2,709 (s), 2,659 (s), 2,649 (s), 2,602 (vs), 2,160 (vs), 1,841 (vs), 1,735 (s), 1,585 (vs), 1,538 (vs), 1,496 (vs), 1,445 (vw), 1,393 (m), 1,369 (w), 1,307 (w), 1,262 (m), 1,254 (m), 1,149 (m), 1,124 (s), 1,093 (w), 1,052 (w), 939 (s), 890 (vw), 843 (m), 828 (m), 810 (s), 758 (m), 744 (m), 697 (vw), 617 (w), 592 (w), 567 (w), 538 (vw), 528 (vw), 510 (vw), 485 (w), 467 (vw), 436 (vw), 407 (vw).

$[LuI_3(THF)_3]$ (**7**). THF (125 mL) was added to a pre-cooled (0°C) 250 mL J. Youngs appended round-bottomed flask, equipped with a PTFE-coated stirrer bar, containing Lu^0 metal filings (5.000g, 28.6 mmol). Solid iodine (10.888, 42.9 mmol) was added in portions against a strong flow of argon to the colourless suspension. The brown mixture was allowed to warm to room temperature. After stirring at room temperature for 3 days the brown mixture was concentrated to *ca*. 30 mL and the supernatant was filtered. The remaining brown solids were washed once with hexane (30 mL) and dried under vacuum (10^{-3} mbar, 8 hours) at room temperature. The grey solids were purified by Soxhlet extraction in THF. The grey solution was concentrated to ca. 50 mL and Et2O (50 mL) followed by pentane (50 mL) was added. The grey suspension was filtered, and the solids dried under vacuum (10^{-3} mbar, 8 hours) yielding $[LuI_3(THF)_3]$ as a grey solid (yield = 20.825 g, 94%).

Elemental analysis on $C_{12}H_{24}O_3I_3Lu$ calc. (%): C = 18.67, H = 3.13, N = 0.00; found (%): C = 18.47, H = 3.11, N = 0.00.

^{1}H NMR (C_6D_6 and C_5D_5N, 400.13 MHz, 298 K): δ = 3.51 (m, 12H, THF *H*), 1.43 (m, 12H, THF *H*).

$^{13}C\{^{1}H\}$ NMR (C_6D_6 and C_5D_5N, 100.62 MHz, 298 K): 67.45 (s, THF *C*), 25.43 (s, THF *C*).

FT-IR (ATR, microcrystalline) cm^{-1} = 2,988 (m), 2,974 (m), 2,953 (m), 2,929 (w), 2,900 (s), 2,875 (m), 2,828 (vw), 1,484 (vw), 1,445 (s), 1,342 (s), 1,295 (vw), 1,245 (m), 1,178 (m), 1,040 (s), 995 (vs), 950 (s), 910 (vs), 826 (vs), 721 (s), 707 (s), 674 (vs), 602 (m), 592 (m), 575 (vs), 549 (w), 536 (w), 526 (w), 516 (vw), 508 (w), 493 (vw), 475 (vw), 458 (w), 448 (vw), 427 (vw), 421 (w), 403 (vw).

3. Results and Discussion

3.1. Synthesis and Spectroscopic Characterisation

The preparation of targeted rare earth phospholide COT complexes first required the rare earth cyclooctatetraenenide complexes [M(COT)(I)(THF)$_n$] (**1M**, M = Sc, Y, Lu, *n* = 2) which were prepared by analogy to previously-reported [M(COT)(I)(THF)$_n$] (M = La, Ce, Pr, n = 3; M = Y, Nd, n = 2; M = Sm, n = 1) from M^0 (M = La, Y) metal filings,[61,64,65] one equivalent of cyclooctatetraene and half an equivalent of iodine at elevated temperatures in THF over several days. The crystal structure of **1Y** has been reported previously, and the metrical parameters are in agreement with our own data which we will use for discussion (see below).[66] In the case of **1Lu**, this reaction failed and only [$LuI_3(THF)_3$] (**7**) could be isolated, the structure of which is reported here for the first time (see *Supporting Information*). Elemental microanalysis and ^{1}H NMR spectroscopy suggest **7** does not readily undergo desolvation under vacuum (10^{-3} mbar) at room temperature. Complexes **1Sc** and **1Lu** were instead synthesised from the reaction between molecular triiodides [$MI_3(THF)_3$] (M = Sc, Lu) and K_2COT (**Scheme 1**).[61] Crystallisation of **1M** complexes from THF gave large yellow blocks suitable for single crystal XRD in fair to excellent yields (49-81%). After drying *under*

vacuum (2 hours at 10^{-3} mbar) elemental microanalysis confirmed that these complexes do not undergo desolvation under the conditions described.

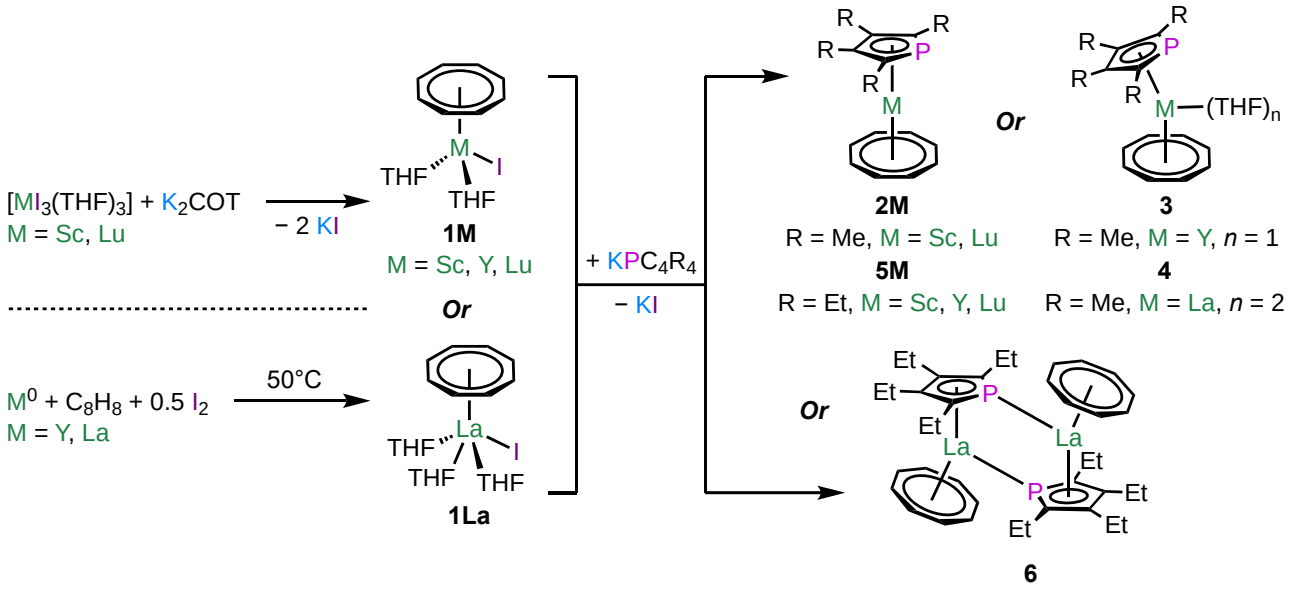

Scheme 1. Synthesis of complexes **1**-**6**.

With **1M** (M = Sc, Y, La, Lu) in hand, we turned our attention to the isolation of phospholide complexes. The addition of THF to a pre-cooled (–98°C) mixture of **1M** and one equivalent of either KTMP (TMP = {PC_4Me_4}) or KTEP (TEP = {PC_4Et_4}) gave white suspensions and pale straw-coloured solutions upon warming to room temperature with stirring overnight (16 hours). The mixtures were reduced to dryness under vacuum (10^{-3} mbar). In the case of [M(COT)(TMP)] (**2M**, M = Sc, Lu), [M(COT)(TEP)] (**5M**, M = Sc, Y, Lu), and [La(COT)(μ-TEP)]$_2$ (**6**), toluene was added followed by a brief period at reflux (<1 minute). The supernatant was filtered at room temperature and concentrated under vacuum. Storage at low temperature (5°C followed by –30°C) gave complexes **2M**, **5M**, and **6** as colourless blocks suitable for single crystal XRD in fair yields (38-58%). In the case of [Y(COT)(TMP)(THF)] (**3**) and [La(COT)(TMP)(THF)$_2$] (**4**), the white solids were found to be insoluble in common non-coordinating solvents (hexane, toluene, benzene) and were

instead crystallised from THF as adducts in poor (**3**, 18%) or good (**4**, 61%) yields (**Scheme 1**).

The ^{1}H NMR spectra for **2**–**6** are characteristic of complexes with these ligand sets[51,67]. The TMP 2,5-Me groups in **2Sc**, **2Lu**, **3**, and **4** present as doublets ($^{3}J_{HP}$ = 10 Hz) spanning a narrow range of ^{1}H shifts (δ_H = 1.76–1.96), while the 3,4-Me singlets appear slightly upfield (δ_H = 1.67–1.89). In complexes **5M** (M = Sc, Y, Lu) and **6**, the CH_3 protons of the TEP 2,5-Et (δ_H = 1.11–1.21) groups are somewhat downfield of the 3,4-Et groups (δ_H = 0.83–1.11) and both sets give typical triplet splitting patterns ($^{3}J_{HH}$ *ca*. 7.5 Hz). The corresponding CH_2 ^{1}H resonances are only well-resolved for **2Lu** where the 3,4-Et CH_2 groups appear as a quartet (δ_H = 2.19; $^{3}J_{HH}$ = 7.6 Hz) and the 2,5-Et CH_2 displays additional coupling to the adjacent ^{31}P and appears as a doublet of quartets (δ_H = 2.34; $^{3}J_{HP}$ = 8.8 Hz, $^{3}J_{HH}$ = 7.6 Hz). The CH_2 groups for the remaining TEP complexes (**5Sc**, **5Y**, **6**) show more complex coupling patterns or broadened features which may arise due to aggregation processes in solution or unresolved long-range coupling to the metal centre (see *Supporting Information*). In complex **3**, the COT ^{1}H resonance appears as a doublet (δ_H = 6.14; $^{2}J_{HY}$ = 1.0 Hz) due to the presence of ^{89}Y (I = $^{1}/_{2}$, 100% natural abundance), while in all other complexes, including **5Y**, the COT group appears as a singlet over a small range (δ_H = 6.24–6.31). While the COT ^{1}H peak shows no coupling to ^{89}Y in **5Y**, the ^{13}C{^{1}H} NMR spectrum shows a doublet for the COT ^{13}C environment (δ_C = 93.90, $^{1}J_{CY}$ = 2.6 Hz) which is almost identical to that of **3** (δ_C = 98.15, $^{1}J_{CY}$ = 2.6 Hz); conversely, only **5Y** shows ^{13}C-^{89}Y coupling to phospholide ring C-atoms, whereby the 2,5- positions appear as a doublet of doublets due to additional ^{13}C-^{31}P coupling (δ_H = 150.54; $^{1}J_{CP}$ = 48.4 Hz, $^{1}J_{CY}$ = 1.0 Hz) – for further information on the ^{13}C{^{1}H} NMR spectra of all complexes, see the *Supporting Information*. The phospholide ligands present a convenient spectroscopic tag through the ^{31}P (I = $^{1}/_{2}$, 100% nat. abund.) nucleus which is also highly sensitive to its local environment[68,69]. The ^{31}P{^{1}H} NMR spectrum of **3**

reveals ^{31}P-^{89}Y coupling (doublet, δ_H = 84.78; $^1J_{PY}$ = 9.0 Hz); however, with **5Y** a more complex feature is seen which resembles a broad triplet (δ_P = 82.28), the cause of which is not currently understood as the ^{89}Y NMR spectrum (see below) does not reveal signs of aggregation. In principle we also could observe M–^{31}P coupling to: ^{45}Sc (I = $^7/_2$, 100% nat. abund.) in **2Sc** and **5Sc**; ^{139}La (I = $^7/_2$, >99% nat. abund.) in **4** and **6**; or ^{175}Lu (I = $^7/_2$, >97% nat. abund.) in **2Lu** and **5Lu**. Despite the presence of these abundant spin-active metal centres, the ^{31}P{^{1}H} NMR spectra for all complexes display a single resonance (*i.e.* do not show coupling to the metal centre), and span a reasonably narrow range (δ_P = 81.36–95.67) with no clear trend between the chemical shift or structural parameters in the solid state (see *Supporting Information*). The ^{45}Sc NMR spectra of **2Sc** and **5Sc** each reveal a single broad resonance at 13.04 ppm and −18.15 ppm respectively, and the ^{89}Y-^{1}H HSQC spectra of **3** and **5Y** reveal ^{89}Y chemical shifts of −155.43 and −91.39 ppm respectively, both arise from coupling to the COT ring protons.

3.2 Structural Characterisation

The solid-state structures of **1M** (M = Sc, Y, Lu), **2M** (M = Sc, Lu), **3**, **4**, **5M** (M = Sc, Y, Lu), **6**, and **7** were determined by single crystal X-ray diffraction (SC-XRD, additional crystallographic data are compiled in the *Supporting Information*). Note that throughout the following section ESDs are not given on distances and angles which involve ring centroids (C_8 or C_4P) as these are not refined positions.

Complex **1Sc** crystallised in the non-centrosymmetric space group P*c* with Z' = 2 whereas **1Y** and **1Lu** crystallised in the centrosymmetric space group P2$_1$/*n* with Z' = 1. The data for **1Y** and **1Lu** were collected at 200 K and 250 K respectively as they were found to undergo phase changes below *ca*. 150 to 200 K, which did not go to completion upon cooling to 100 K (the low temperature limit of our instrument). While this process was reversible in the case

of **1Y**, reverting to a pure phase up warming to 300 K, in the case of **1Lu** the phase change was irreversible with little to no change observe when warming from 100 K back to 300 K.

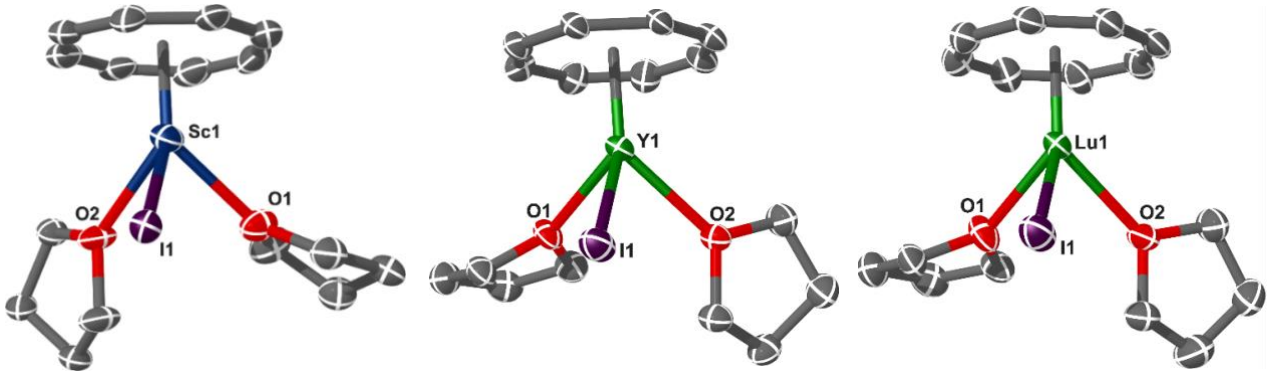

Figure 2. Molecular structure of [M(COT)(I)(THF)$_2$] **1M** (M = Sc, Y, Lu). Ellipsoids set at 30% probability and H-atoms and disordered components have been removed for clarity (operations: X, Y, Z).

The structures of **1M** (M = Sc, Y, Lu) are shown in **Figure 2** and all feature an η^8-COT ring, two coordinating THF molecules and an iodide in a *pseudo*-tetrahedral arrangement which is similar to [La(COT)(I)(THF)$_3$], although the latter has three coordinating THF molecules[63]. The M···C$_{8\text{-centroid}}$ distances range from 1.646(12) Å to 1.834(12) Å and follow the expected trend based on Lewis acidity / trivalent ionic radius (6-coordinate: Sc = 0.745 Å; Lu = 0.861 Å; Y = 0.900 Å; La = 1.032 Å)[70] and are similar to other [M(COT)(I)(donor)$_n$] complexes in the literature, accounting for differences in the ionic radius of the metal ion[63-66,71-77]. It is interesting to note that while the M···C$_{8\text{-centroid}}$ distance in **1Sc** compares well to that of [Sc(COT)(Cl)(DME)] (1.600 Å), both are significantly longer than in dimeric [Sc$_2$(C$_8$H$_6$-1,4-TMS$_2$)$_2$(μ-Cl)$_2$(μ-thf)] (1.535 and 1.550 Å), possibly due to the larger number of Sc–anion contacts in the latter which reduces the charge density at Sc[78], though in the related complex, [Sc(C$_8$H$_8$)(μ-Cl)(THF)]$_2$, the same distance is 1.597 Å[79]. The C$_{8\text{-centroid}}$···M···I angle remains essentially invariant across the **1M** complexes[61,70]. Selected bond lengths and angles for **1M** are summarised in **Table 1**.

Table 1. Selected bond distances (Å) and angles (°) for **1M**.

	M–I (Å)	M–O(1) (Å)	M–O(2) (Å)	M···$C_{8\text{-centroid}}$ (Å)	$C_{8\text{-centroid}}$···M···I (°)
1Sc	2.983(9)	2.23(2)	2.286(19)	1.646	130.1
1Lu	3.008(5)	2.330(11)	2.351(14)	1.748	132.2
1Y	3.0614(6)	2.35(2)	2.384(11)	1.834	130.4

The TMP complexes **2M** (M = Sc, Lu), **3**, **4** all crystallised in the centrosymmetric space group $P2_1/c$ with $Z' = 1$ except for **4** ($Z' = 2$), and their molecular structures are shown in **Figure 3** in the order of increasing metal ionic radius (Sc < Lu < Y < La). All four feature an η^8-COT ring and an η^5-TMP ring with the metal coordination spheres in **3** and **4** completed by one or two coordinated THF molecules respectively.

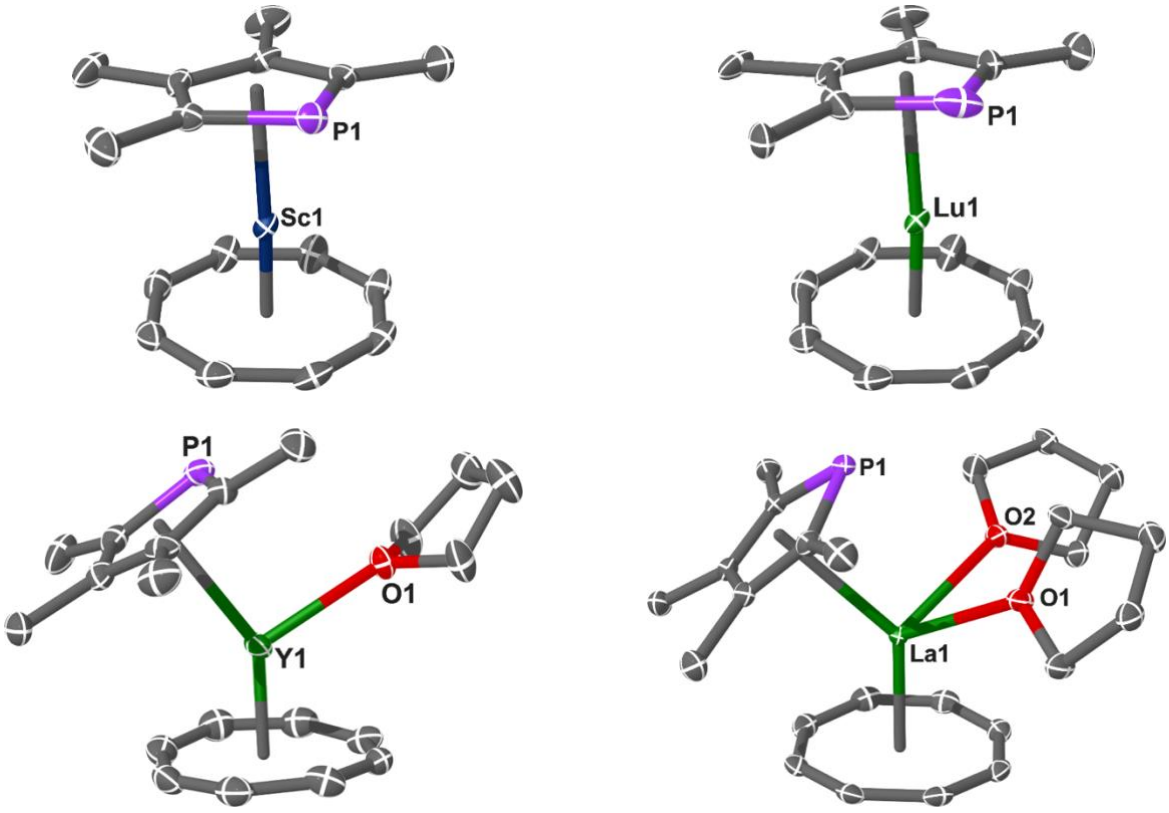

Figure 3. Molecular structures of [Sc(COT)(TMP)] (**2Sc**), [Lu(COT)(TMP)] (**2Lu**), [Y(COT)(TMP)(THF)] (**3**), and [La(COT)(TMP)$(THF)_2$] (**4**). Ellipsoids set at 50% probability,

and H-atoms and disordered components have been removed for clarity (operations: X, Y, Z).

Both the M···$C_{8\text{-centroid}}$ distances in **2Sc** (1.5031 Å) and **2Lu** (1.628 Å), and the M···$C_4P_{centroid}$ distances (2.129 Å in **2Sc** to 2.262 Å in **2Lu**) follow the expected trend based on their respective 6-coordinate trivalent ionic radii ($\Delta_{M\cdots C8\text{-centroid}}$ = 0.1249 Å; $\Delta_{M\cdots C4P\text{-centroid}}$ = 0.133 Å; Δ_{rad} = 0.116 Å) and the $C_{8\text{-centroid}}$···M···$C_4P_{centroid}$ angles decrease from 174.14° in **2Sc** to 172.219° in **2Lu**[70]. The M···$C_{8\text{-centroid}}$ distances in **3** and **4** increase significantly from 1.783 Å in **3** to 2.0748 Å **4** as well as the M···$C_4P_{centroid}$ distances which increase from 2.395 Å in **3** to 2.6946 Å in **4** – though, again, these differences are broadly in line with the differences in their respective ionic radii (Δ_{rad} = 0.132)[70], with the remainder likely due to the difference in their formal coordination numbers. The $C_{8\text{-centroid}}$···M···$C_4P_{centroid}$ angles decrease from (2.395 Å in **3** to 2.6946 Å in **4**). The greater changes in bond metrics between **3** and **4** can be attributed to the coordination of an additional molecule of THF in **4** compared to **3**. Selected bond distances and angles for complexes **2M**, **3** and **4** are summarised in **Table 2**.

Table 2. Selected bond distances (Å) and angles (°) for **2M**, **3** and **4**.

	M–P(Å)	**M···$C_4P_{centroid}$ (Å)**	**M···$C_{8\text{-centroid}}$ (Å)**	**$C_4P_{centroid}$···M···$C_{8\text{-centroid}}$ (°)**
2Sc	2.631(2)	2.129	1.5031	174.14
2Lu	2.735(8)	2.262	1.628	172.22
3	2.853(3)	2.395	1.783	144.38
4	3.0632(4)	2.6946	2.0748	135.32

Complexes **5Y** and **5Lu** crystallised in P*bca* with *Z*′ = 1, and **5Sc** crystallised in $P2_1/n$ with *Z*′ = 1 and an additional molecule of toluene – note that all three were crystallised from

toluene. Complex **6** crystallised as a centrosymmetric dimer (Z' = 0.5) in C2/*c*. The molecular structures of **5M** (M = Sc, Lu, Y), and **6** are shown in **Figure 4**.

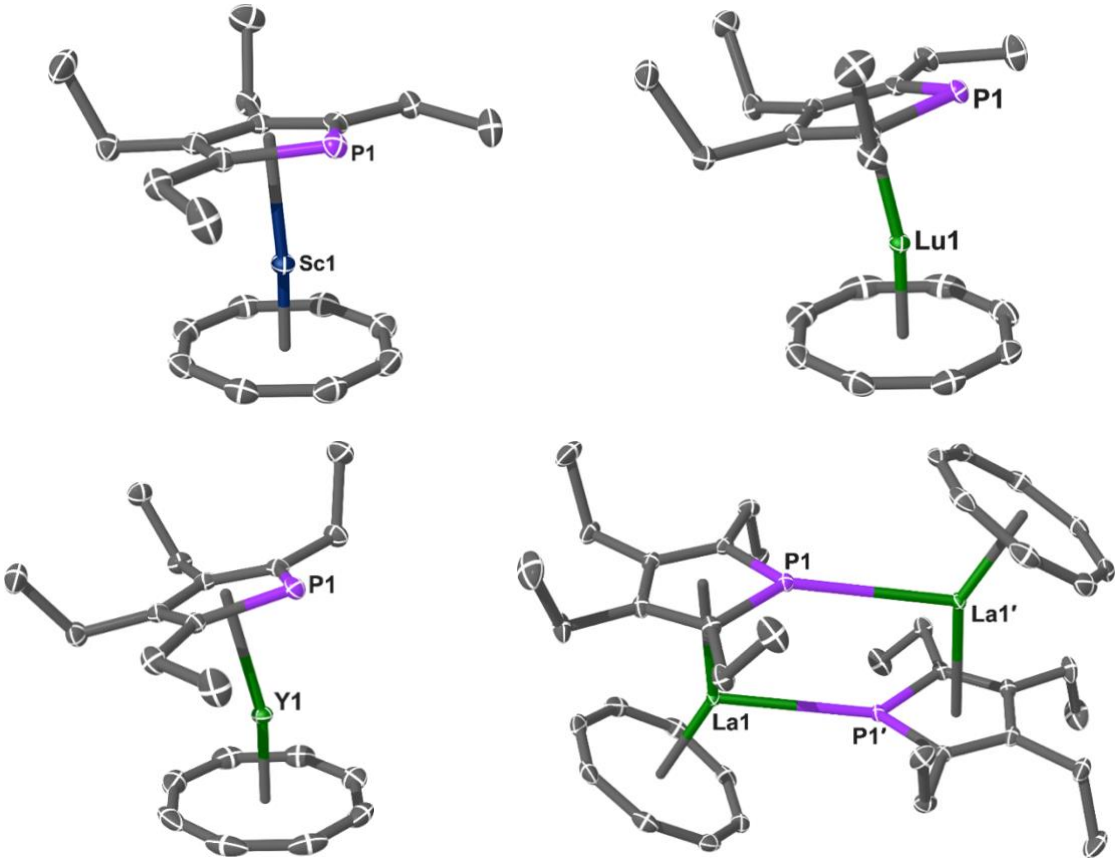

Figure 4. Molecular structures of [Sc(COT)(TMP)] (**5Sc**), [Lu(COT)(TEP)] (**5Lu**), [Y(COT)(TEP)] (**5Y**), and [La(COT)(μ-TEP)]$_2$ (**6**). Ellipsoids set at 50% probability, and H-atoms and disordered components have been removed for clarity (operations for **5M**: X, Y, Z; operations for **6**: X, Y, Z; 3/2−X, 1/2−Y, 1−Z).

The three **5M** complexes along with **6** feature η^8-COT rings along with an η^5-TEP ring, while **6** presents an additional bond between the TEP P-atom lone pair on one {La(COT)(TEP)} unit to a second La metal centre (La–P = 3.1781(3) Å). This interaction is similar to the dimeric arsolide COT complex [Sm(COT)(μ-TMAs)]$_2$ (TMAs = {AsC$_4$Me$_4$})[67], and also the silole complex [La{(μ-COT)K(THF)$_2$}(μ-SiC$_4$-2,5-TMS-3,4-Ph)]$_2$[80], but contrasts other examples such as [Nd(COT)(TMP)(HMPA)] (HMPA = OP(NMe$_2$)$_3$), [Er(COT)(DSP)], and

[Nd(COT)(DSP)(THF)] which are monomeric[51,54,67,81]. In **5Sc**, two of the ethyl groups lie in the plane of the TEP ring, somewhat sterically shielding the P-atom, and the other two point away from the metal, whereas in **5Lu** and **5Y** three point away from the metal and one lies in the plane of the ring. Complex **6** is the outlier where three ethyl groups point away from the metal while the fourth points inwards, towards the La centre. The M···$C_{8\text{-centroid}}$ distances in **5M** range from 1.4997 Å in **5Sc** to 1.701 Å in **5Y**, then 2.0031 Å in **6**. The difference between **5Y** and **6** is larger than the difference in their ionic radii, though **6** has a higher formal coordination number. The M···$C_4P_{centroid}$ distances display a similar trend from 2.1480 Å in **5Sc** to 2.3555 Å in **5Y**, while the equivalent distance in **6** is elongated significantly (2.6328 Å). The $C_{8\text{-centroid}}$···M···$C_4P_{centroid}$ angles decrease from 174.01° in **5Sc** to 164.49° in **5Y**.[70] Selected distances and angles for **5M** and **6** are summarised in **Table 3**.

Table 3. Selected bond distances (Å) and angles (°) for **5M** and **6**.

	M–P(Å)	**M···$C_4P_{centroid}$ (Å)**	**M···$C_{8\text{-centroid}}$ (Å)**	**$C_4P_{centroid}$···M···$C_{8\text{-centroid}}$ (°)**
5Sc	2.6774(4)	2.1480	1.4997	174.01
5Lu	2.7640(7)	2.2820	1.641	168.11
5Y	2.8270(3)	2.3555	1.701	164.49
6	3.0523(5) 3.1781(3) [A]	2.6328	2.0031	144.76

[A] Bridging La–P distance.

The Sc(III) and Lu(III) complexes in the **2M** and **5M** series are both monomeric base-free sandwich complexes and so their structures allow a comparison between the steric differences between the TMP and TEP ligand sets – though we cannot account for differences in crystal packing forces. Upon comparing the M–P bond distances in the two Sc(III) complexes, we find an increase from 2.631(2) Å in **2Sc** to 2.6774(4) Å in **5Sc**, though

any change in the $C_4P\cdots Sc\cdots C_{8\text{-centroid}}$ angle does not reach statistical significance, and so the M–P lengthening instead is a manifestation of the larger $Sc\cdots C_4P$ centroid distance in **5Sc** (2.1480 Å) than in **2Sc** (2.129 Å). That is to say, the ethyl groups in the TEP ligand appear to site the C_4P ring further from the metal, rather than simply inducing increased (or decreased) co-planarity of the two arene rings. Comparing the M–P distances in the two Lu(III) complexes, we find an increase from 2.735(8) Å in **2Lu** to 2.7640(7) Å in **5Lu**, which again is accompanied by an increase in the $M\cdots C_4P_{centroid}$ distance from 2.262 Å (**2Lu**) to 2.2820 (**5Lu**), but this time the complex becomes slightly more bent, with the $C_4P_{centroid}\cdots Lu\cdots C_{8\text{-centroid}}$ angle decreasing from 172.22° in **2Lu** to 168.11° in **5Lu**.

Unlike the Sc(III) and Lu(III) **2M** and **5M** complexes above, the M–P distances in TMP complexes **3** (2.853(3) Å) and **4** (3.0632(4) Å) are longer than in **5Y** (2.8270(3) Å) and **6** (3.0523(5) Å). This reflects the higher formal coordination numbers in **3** and **4** due to coordination of one or two THF moieties respectively. The increased M–P bond lengths are also reflected in the longer $C_4P_{centroid}\cdots M$ distances in **3** and **4** than **5Y** and **6**. The TEP complexes **5Y** and **6** feature larger $C_4P_{centroid}\cdots M\cdots C_{8\text{-centroid}}$ angles as the THF units force this angle open in **3** and **4** – though it is interesting that in **3**, which features a single additional Lewis-basic unit coordinated to the metal, the angle (144.38°) is similar to that of **6** (144.76°) which also has just one additional Lewis-base bound to the metal.

Reflecting the dearth of phospholide chemistry in general, there are few structurally characterised rare earth complexes using either the TMP or TEP ligand sets with which to compare the M–P bond lengths. However, Tilley previously reported $[Sc(TMP)_2(\mu\text{-}Cl)_2Li(TMEDA)]$ which has Sc–P distances (2.694(2) and 2.718(2) Å) that are somewhat longer than in **2Sc**, presumably as the second TMP ligand provides greater steric crowding than the COT ligand in **2Sc**[19]. For the larger rare earths, the nearest comparisons are

$[La(TMP)_2(\mu{:}\eta^1{:}\eta^6\text{-}C_7H_7)_2K(\eta^6\text{-}C_7H_8)]$ (La–P = 3.0407(15) and 3.0112(12) Å)[82], and [Nd(COT)(TMP)(HMPA)] (Nd–P = 2.968(8) Å)[81] which both compare well to **4** (3.0632(4) Å) and **6** (3.0523(5) Å) once differences in the ionic radii of La(III) (1.032 Å) and Nd(III) (0.983 Å; Δ = 0.049 Å) are accounted for[70]. In the case of dimeric **6**, the $La–P_{bridging}$ distance (3.1781(3) Å) is shorter than the equivalent distance in $[La(\mu\text{-}TMP)(AlMe_4\text{-}\kappa^2\textit{Me},\textit{Me})_2]_2$ (3.1962(3) Å)[50], though the latter has a higher formal coordination number. Accounting for the difference in the ionic radius of 8-coordinate La(III) (1.160 Å) *vs* the 6-coordinate value (1.032 Å), the difference in $La–P_{bridging}$ bond lengths ($\Delta_{La–P}$ = 0.0181(4) Å) is negligible.

It is interesting to note that only **6** was isolated as a dimer through coordination of the P-atom lone pair on one TEP ring to a second La(III) metal centre, whereas in the case of the TMP analogue, **4**, the complex is monomeric but contains two THF molecules bound to the La(III) metal centre. In a similar fashion, complex **5Y** is monomeric and free of Lewis basic co-ligands, while **3** features a THF molecule bound to the Y(III) metal centre. It is likely that the poor solubility of TMP complexes **3** and **4** in non-coordinating solvents is due to their existence as dimeric (or higher order) species in the solid-state, except in the presence of an excess of a Lewis base (THF) to produce solvated monomers. Conversely, the slightly increased steric bulk of TEP possibly hinders dimer formation somewhat, but it may also significantly increase the solubility of the complexes and so **5Y** could be extracted into non-coordinating solvents and crystallised without the presence of additional Lewis base coordination. This increased bulk is clearly not sufficient to preclude dimer formation with La(III) in **6**. That the $M–P_{bridging}$ distance in **6** is shorter than in $[La(\mu\text{-}TMP)(AlMe_4\text{-}\kappa^2\textit{Me},\textit{Me})_2]_2$ lends credence to the argument that the different behaviour of the TMP and TEP ligand systems likely derives from crystal packing and solubility differences, rather than notable differences in their steric demands, though this requires further investigation.

4. Conclusion

To summarise, we have described the synthesis and molecular structures of a series of crystalline heteroleptic rare earth phospholide COT sandwich complexes using Sc(III), Y(III), La(III), and Lu(III) and employing two different per-alkylated phospholide ligands: {PC_4Me_4} (TMP) and {PC_4Et_4} (TEP). In addition to their molecular structures, these complexes have been characterised by ATR-IR, UV-Vis-NIR, and multinuclear NMR spectroscopy (^{1}H, ^{13}C, ^{31}P, ^{45}Sc, ^{89}Y, as appropriate). The title complexes were isolated from salt elimination reactions between KTMP or KTEP salts, and monomeric [M(COT)(I)$(THF)_n$] precursors (**1M**; M = Sc, Y, Lu, *n* = 2; M = La, *n* = 3). The synthesis and molecular structures of **1Sc** and **1Lu** are reported here for the first time, and **1Y** was only recently reported[66]. During the course of this work, we have also determined the molecular structure of $[LuI_3(THF)_3]$ (**7**) for the first time.

With the smaller rare earth ions Sc(III) and Lu(III), both TMP and TEP ligands gave monomeric sandwich complexes of the form [M(COT)(PC_4R_4)] (R = Me, **2M**, M = Sc, Lu; or R = Et, **5M**, M = Sc, Lu) when crystallised from toluene. With the larger Y(III) ion, the smaller TMP ligand gave a poorly soluble species which could only be extracted into and crystallised from THF and hence formed the Lewis base adduct [Y(COT)(TMP)(THF)] (**3**), presumably due to oligomerisation in the solid state in the absence of THF. In a similar fashion, the La(III) complex with TMP was isolated from THF as a *bis*-THF adduct [La(COT)(TMP)$(THF)_2$] (**4**). With the larger TEP ligand, a Y(III) complex was isolated free of THF coordination in monomeric [Y(COT)(TEP)] (**5Y**), whereas the La(III) analogue was found to crystallise as dimeric [La(COT)(μ-TEP)] (**6**). These differences can be attributed to small differences in the steric profile of TMP *vs* TEP, though we suspect this is eclipsed by differences in their crystal packing and solubility profiles. With the basic coordination chemistry of these ligand

sets on diamagnetic rare earths established, work in our laboratory to better understand their behaviour with actinide elements is ongoing.

Acknowledgements

We thank the Royal Society for a University Research Fellowship (URF\211271 to C.A.P.G and part-funding for D. J. O.). We acknowledge funding from the EPSRC (EP/K039547/1, EP/V007580/1, EP/P001386/1, and EP/K039547/1 for NMR spectroscopy and X-ray diffraction) and the EPSRC DTP EP/W524347/1 studentships (C. N. D. and D. J. O). Elemental analyses were performed at the UoM by Mr Martin Jennings and Ms Anne Davies.

Author contributions: CRediT

CND: Investigation, data curation, formal analysis, visualisation, writing – original draft. **DJO**: Investigation. **RWA**: Investigation, formal analysis, methodology. **GFSW**: Data curation, formal analysis, validation. **CAPG**: Conceptualisation, formal analysis, methodology, project administration, supervision, writing – review and editing.

Declaration of competing interest

The authors declare no competing financial interest.

Supplementary Materials

The following CCDC references contain the supplementary crystal data for this article: **1Sc** (2364920), **1Y** (2364921), **1Lu** (2364922), **2Sc** (2364923), **2Lu** (2364924), **3** (2364925), **4** (2364926), **5Sc** (2364927), **5Y** (2364928), **5Lu** (2364929), **6** (2364930), and **7** (2364931). These data can be obtained free of charge from the Cambridge Crystallographic Data Centre via www.ccdc.cam.ac.uk/data_request/cif. Raw experimental data (NMR, ATR-IR,

UV-Vis-NIR, SQUID Magnetometry) and computational inputs/outputs can be found freely at DOI: 10.48420/XXXX. {{Embargoed until publication}} The authors have cited additional references within the *Supporting Information*[83-93].

5. References

(1) Aspinall, H. C. Chiral Lanthanide Complexes: Coordination Chemistry and Applications. *Chem. Rev.* **2002**, *102*, 1807-1850. DOI: https://doi.org/10.1021/cr010288q

(2) Benner, F.; Delano, F.; R Pugliese, E.; Demir, S. 4.04 - Cyclopentadienyls and Phospholyls of the Group 3 Metals and Lanthanides. In *Comprehensive Organometallic Chemistry IV*, Parkin, G., Meyer, K., O'hare, D. Eds.; Elsevier, 2022; pp 98-184.

(3) Gremillion, A. J.; Walensky, J. R. 4.05 - Cyclopentadienyl and phospholyl compounds in organometallic actinide chemistry. In *Comprehensive Organometallic Chemistry IV*, Parkin, G., Meyer, K., O'hare, D. Eds.; Elsevier, 2022; pp 185-247.

(4) Stetsiuk, O.; Cemortan, V.; Simler, T.; Nocton, G. 4.10 - Larger Aromatic Complexes of the Group 3 Metals and Lanthanides. In *Comprehensive Organometallic Chemistry IV*, Parkin, G., Meyer, K., O'hare, D. Eds.; Elsevier, 2022; pp 550-581.

(5) Walter, O. 4.11 - Larger Aromatic Complexes of the Actinides☆. In *Comprehensive Organometallic Chemistry IV*, Parkin, G., Meyer, K., O'hare, D. Eds.; Elsevier, 2022; pp 582-606.

(6) Resa, I.; Carmona, E.; Gutierrez-Puebla, E.; Monge, A. Decamethyldizincocene, a stable compound of Zn(I) with a Zn-Zn bond. *Science* **2004**, *305*, 1136-1138. DOI: https://doi.org/10.1126/science.1101356

(7) Boronski, J. T.; Seed, J. A.; Hunger, D.; Woodward, A. W.; van Slageren, J.; Wooles, A. J.; Natrajan, L. S.; Kaltsoyannis, N.; Liddle, S. T. A crystalline tri-thorium cluster

with σ-aromatic metal-metal bonding. *Nature* **2021**, *598*, 72-75. DOI: https://doi.org/10.1038/s41586-021-03888-3

(8) Boronski, J. T.; Crumpton, A. E.; Wales, L. L.; Aldridge, S. Diberyllocene, a stable compound of Be(I) with a Be-Be bond. *Science* **2023**, *380*, 1147-1149. DOI: https://doi.org/10.1126/science.adh4419

(9) Gould, C. A.; McClain, K. R.; Reta, D.; Kragskow, J. G. C.; Marchiori, D. A.; Lachman, E.; Choi, E.-S.; Analytis, J. G.; Britt, R. D.; Chilton, N. F.; Harvey, B. G.; Long, J. R. Ultrahard magnetism from mixed-valence dilanthanide complexes with metal-metal bonding. *Science* **2022**, *375*, 198-202. DOI: https://doi.org/10.1126/science.abl5470

(10) Goodwin, C. A. P.; Ortu, F.; Reta, D.; Chilton, N. F.; Mills, D. P. Molecular magnetic hysteresis at 60 kelvin in dysprosocenium. *Nature* **2017**, *548*, 439-442. DOI: https://doi.org/10.1038/nature23447

(11) Goodwin, C. A. P.; Reta, D.; Ortu, F.; Chilton, N. F.; Mills, D. P. Synthesis and Electronic Structures of Heavy Lanthanide Metallocenium Cations. *J. Am. Chem. Soc.* **2017**, *139*, 18714-18724. DOI: https://doi.org/10.1021/jacs.7b11535

(12) Guo, F.-S.; Day, B. M.; Chen, Y.-C.; Tong, M.-L.; Mansikkamäki, A.; Layfield, R. A. Magnetic hysteresis up to 80 kelvin in a dysprosium metallocene single-molecule magnet. *Science* **2018**, *362*, 1400-1403. DOI: https://doi.org/10.1126/science.aav0652

(13) Gould, C. A.; McClain, K. R.; Yu, J. M.; Groshens, T. J.; Furche, F.; Harvey, B. G.; Long, J. R. Synthesis and Magnetism of Neutral, Linear Metallocene Complexes of Terbium(II) and Dysprosium(II). *J. Am. Chem. Soc.* **2019**, *141*, 12967-12973. DOI: https://doi.org/10.1021/jacs.9b05816

(14) Kahan, R. J.; Cloke, F. G. N.; Roe, S. M.; Nief, F. Activation of carbon dioxide by new mixed sandwich uranium(III) complexes incorporating cyclooctatetraenyl and

pyrrolide, phospholide, or arsolide ligands. *New J. Chem.* **2015**, *39*, 7602-7607. DOI: https://doi.org/10.1039/C5NJ00590F

(15) Kahan, R. J.; Farnaby, J. H.; Tsoureas, N.; Cloke, F. G. N.; Hitchcock, P. B.; Coles, M. P.; Roe, S. M.; Wilson, C. Sterically encumbered mixed sandwich compounds of uranium(III): Synthesis and reactivity with small molecules. *J. Organomet. Chem.* **2018**, *857*, 110-122. DOI: https://doi.org/10.1016/j.jorganchem.2017.10.038

(16) Summerscales, O. T.; Cloke, F. G. N.; Hitchcock, P. B.; Green, J. C.; Hazari, N. Reductive Cyclotrimerization of Carbon Monoxide to the Deltate Dianion by an Organometallic Uranium Complex. *Science* **2006**, *311*, 829-831. DOI: https://doi.org/10.1126/science.1121784

(17) Evans, W. J.; Ulibarri, T. A.; Ziller, J. W. Isolation and x-ray crystal structure of the first dinitrogen complex of an f-element metal, $[(C_5Me_5)_2Sm]_2N_2$. *J. Am. Chem. Soc.* **1988**, *110*, 6877-6879. DOI: https://doi.org/10.1021/ja00228a043

(18) Chen, S.; Yan, D.; Xue, M.; Hong, Y.; Yao, Y.; Shen, Q. Tris(cyclopentadienyl)lanthanide Complexes as Catalysts for Hydroboration Reaction toward Aldehydes and Ketones. *Org. Lett.* **2017**, *19*, 3382-3385. DOI: https://doi.org/10.1021/acs.orglett.7b01335

(19) Fontaine, F. G.; Tupper, K. A.; Tilley, T. D. Synthesis, characterization and reactivity of tetramethylphospholyl complexes of scandium. *J. Organomet. Chem.* **2006**, *691*, 4595-4600. DOI: https://doi.org/10.1016/j.jorganchem.2006.06.042

(20) Mas-Roselló, J.; Herraiz, A. G.; Audic, B.; Laverny, A.; Cramer, N. Chiral Cyclopentadienyl Ligands: Design, Syntheses, and Applications in Asymmetric Catalysis. *Angew. Chem., Int. Ed.* **2021**, *60*, 13198-13224. DOI: https://doi.org/10.1002/anie.202008166

(21) Panda, T. K.; Zulys, A.; Gamer, M. T.; Roesky, P. W. Cyclooctatetraene Complexes of Yttrium and the Lanthanides with Bis(phosphinimino)methanides: Synthesis,

Structure, and Hydroamination/Cyclization Catalysis. *Organometallics* **2005**, *24*, 2197-2202. DOI: https://doi.org/10.1021/om0491138

(22) Evans, W. J. Tutorial on the Role of Cyclopentadienyl Ligands in the Discovery of Molecular Complexes of the Rare-Earth and Actinide Metals in New Oxidation States. *Organometallics* **2016**, *35*, 3088-3100. DOI: https://doi.org/10.1021/acs.organomet.6b00466

(23) Inman, C. J.; Cloke, F. G. N. The experimental determination of Th(IV)/Th(III) redox potentials in organometallic thorium complexes. *Dalton Trans.* **2019**, *48*, 10782-10784. DOI: https://doi.org/10.1039/C9DT01553A

(24) Geiger, W. E. Electroreduction of cobaltocene. Evidence for a metallocene anion. *J. Am. Chem. Soc.* **1974**, *96*, 2632-2634. DOI: https://doi.org/10.1021/ja00815a062

(25) Holloway, J. D. L.; Bowden, W. L.; Geiger, W. E. Unusual electron-transfer processes involving electron-rich and electron-deficient metallocenes. *J. Am. Chem. Soc.* **1977**, *99*, 7089-7090. DOI: https://doi.org/10.1021/ja00463a066

(26) Connelly, N. G.; Geiger, W. E. Chemical Redox Agents for Organometallic Chemistry. *Chem. Rev.* **1996**, *96*, 877-910. DOI: https://doi.org/10.1021/cr940053x

(27) Malischewski, M.; Adelhardt, M.; Sutter, J.; Meyer, K.; Seppelt, K. Isolation and structural and electronic characterization of salts of the decamethylferrocene dication. *Science* **2016**, *353*, 678-682. DOI: https://doi.org/10.1126/science.aaf6362

(28) Malischewski, M.; Seppelt, K. Structural characterization of potassium salts of the decamethylmanganocene anion $Cp^*_2Mn^-$. *Dalton Trans.* **2019**, *48*, 17078-17082. DOI: https://doi.org/10.1039/c9dt03551f

(29) Goodwin, C. A. P.; Giansiracusa, M.; Greer, S. M.; Nicholas, H. M.; Evans, P.; Vonci, M.; Hill, S.; Chilton, N. F.; Mills, D. P. Isolation and electronic structures of derivatized manganocene, ferrocene and cobaltocene anions. *Nat. Chem.* **2020**, *13*, 243-248. DOI: https://doi.org/10.1038/s41557-020-00595-w

(30) Wilkinson, G.; Rosenblum, M.; Whiting, M. C.; Woodward, R. B. The Structure of Iron Bis-Cyclopentadienyl. *J. Am. Chem. Soc.* **1952**, *74*, 2125-2126. DOI: https://doi.org/10.1021/ja01128a527

(31) Streitwieser, A.; Mueller-Westerhoff, U. Bis(cyclooctatetraenyl)uranium (uranocene). A new class of sandwich complexes that utilize atomic f orbitals. *J. Am. Chem. Soc.* **1968**, *90*, 7364-7364. DOI: https://doi.org/10.1021/ja01028a044

(32) Harder, S.; Prosenc, M. H. The Simplest Metallocene Sandwich: the Lithocene Anion. *Angew. Chem., Int. Ed.* **1994**, *33*, 1744-1746. DOI: https://doi.org/10.1002/anie.199417441

(33) Schumann, H.; Meese-Marktscheffel, J. A.; Esser, L. Synthesis, Structure, and Reactivity of Organometallic π-Complexes of the Rare Earths in the Oxidation State Ln^{3+} with Aromatic Ligands. *Chem. Rev.* **1995**, *95*, 865-986. DOI: https://doi.org/10.1021/cr00036a004

(34) Pool, J. A.; Lobkovsky, E.; Chirik, P. J. Hydrogenation and cleavage of dinitrogen to ammonia with a zirconium complex. *Nature* **2004**, *427*, 527-530. DOI: https://doi.org/10.1038/nature02274

(35) Chirik, P. J. Group 4 Transition Metal Sandwich Complexes: Still Fresh after Almost 60 Years. *Organometallics* **2010**, *29*, 1500-1517. DOI: https://doi.org/10.1021/om100016p

(36) Ephritikhine, M. Recent Advances in Organoactinide Chemistry As Exemplified by Cyclopentadienyl Compounds. *Organometallics* **2013**, *32*, 2464-2488. DOI: https://doi.org/10.1021/om400145p

(37) Zhang, P.; Sadler, P. J. Advances in the design of organometallic anticancer complexes. *J. Organomet. Chem.* **2017**, *839*, 5-14. DOI: https://doi.org/10.1016/j.jorganchem.2017.03.038

(38) Goodwin, C. A. P.; Su, J.; Stevens, L. M.; White, F., D.; Anderson, N. H.; Auxier II, J. D.; Albrecht-Schönzart, T. E.; Batista, E. R.; Briscoe, S. F.; Cross, J. N.; Evans, W. J.; Gaiser, A. N.; Gaunt, A. J.; James, M. R.; Janicke, M. T.; Jenkins, T. F.; Jones, Z. R.; Kozimor, S. A.; Scott, B. L.; Sperling, J. M.; Windorff, C. J.; Yang, P.; Ziller, J. W. Isolation and Characterization of a Californium Metallocene. *Nature* **2021**, *599*, 421-424. DOI: https://doi.org/10.1038/s41586-021-04027-8

(39) Schafer, S.; Kaufmann, S.; Rosch, E. S.; Roesky, P. W. Divalent metallocenes of the lanthanides - a guideline to properties and reactivity. *Chem. Soc. Rev.* **2023**, *52*, 4006-4045. DOI: https://doi.org/10.1039/D2CS00744D

(40) Mathey, F. The chemistry of phospha- and polyphosphacyclopentadienide anions. *Coord. Chem. Rev.* **1994**, *137*, 1-52. DOI: https://doi.org/10.1016/0010-8545(94)03000-G

(41) Le Floch, P. Phosphaalkene, phospholyl and phosphinine ligands: New tools in coordination chemistry and catalysis. *Coord. Chem. Rev.* **2006**, *250*, 627-681. DOI: https://doi.org/10.1016/j.ccr.2005.04.032

(42) Groom, C. R.; Bruno, I. J.; Lightfoot, M. P.; Ward, S. C. The Cambridge Structural Database. *Acta Crystallogr. B* **2016**, *72*, 171-179. DOI: https://doi.org/10.1107/S2052520616003954

(43) Nief, F.; Mathey, F.; Ricard, L.; Robert, F. Coordination chemistry of the new 2,3,4,5-tetramethylphospholyl (C_4Me_4P) π-ligand. Crystal and molecular structure of (η^5-$C_4Me_4P)_2ZrCl_2 \cdot {}^1/_2C_{10}H_8$. *Organometallics* **1988**, *7*, 921-926. DOI: https://doi.org/10.1021/om00094a021

(44) Nief, F.; Mathey, F. A new application of the tetramethylphospholyl (η^5-C_4Me_4P) π-ligand. Synthesis of η^5-tetramethylphospholyl complexes of yttrium and lutetium. *J. Chem. Soc., Chem. Commun.* **1989**, 800-801. DOI: https://doi.org/10.1039/C39890000800

(45) Nief, F.; Ricard, L.; Mathey, F. Phospholyl (phosphacyclopentadienyl) and arsolyl (arsacyclopentadienyl) complexes of ytterbium(II) and samarium(II). Synthetic, structural and multinuclear (^{31}P and ^{171}Yb) NMR studies. *Polyhedron* **1993**, *12*, 19-26. DOI: https://doi.org/10.1016/S0277-5387(00)87048-5

(46) Nief, F.; Riant, P.; Ricard, L.; Desmurs, P.; Baudry-Barbier, D. Synthesis and Reactivity of Bis(phospholyl)neodymium(III) and -samarium(III) Chlorides and Alkyl Derivatives. *Eur. J. Inorg. Chem.* **1999**, 1041-1045. DOI: https://doi.org/10.1002/(SICI)1099-0682(199906)1999:6%3C1041::AID-EJIC1041%3E3.0.CO;2-E

(47) Nief, F.; Ricard, L. Synthesis and Molecular Structure of Bis(pentamethylcyclopentadienyl) Phospholyl- and Arsolylsamarium(III) Complexes: Influence of Steric and Electronic Factors. *Organometallics* **2001**, *20*, 3884-3890. DOI: https://doi.org/10.1021/om010317n

(48) Nief, F.; Turcitu, D.; Ricard, L. Synthesis and structure of phospholyl- and arsolylthulium(II) complexes. *Chem. Commun.* **2002**, *2*, 1646-1647. DOI: https://doi.org/10.1039/b204337h

(49) Nief, F.; de Borms, B. T.; Ricard, L.; Carmichael, D. New Complexes of Divalent Thulium with Substituted Phospholyl and Cyclopentadienyl Ligands. *Eur. J. Inorg. Chem.* **2005**, *2005*, 637-643. DOI: https://doi.org/10.1002/ejic.200400784

(50) Le Roux, E.; Nief, F.; Jaroschik, F.; Törnroos, K. W.; Anwander, R. Mono-phosphacyclopentadienyl bis(tetramethylaluminate) lanthanide complexes. *Dalton Trans.* **2007**, 4866-4870. DOI: https://doi.org/10.1039/b709633j

(51) Visseaux, M.; Nief, F.; Ricard, L. Synthesis of mixed phospholyl/cyclooctatetraenyl–lanthanide complexes. Crystal and molecular structure of (cyclooctatetraenyl)[3,4-dimethyl-2,5-bis (trimethylsilyl)-phospholyl](tetrahydrofuran) neodymium. *J.*

Organomet. Chem. **2002**, *647*, 139-144. DOI: https://doi.org/10.1016/S0022-328X(01)01402-4

(52) Mills, D. P.; Evans, P. f-Block Phospholyl and Arsolyl Chemistry. *Chem. Eur. J.* **2021**, *27*, 6645-6665. DOI: https://doi.org/10.1002/chem.202005231

(53) Evans, P.; Reta, D.; Whitehead, G. F. S.; Chilton, N. F.; Mills, D. P. Bis-monophospholyl dysprosium cation showing magnetic hysteresis at 48 K. *J. Am. Chem. Soc.* **2019**, *141*, 19935-19940. DOI: https://doi.org/10.1021/jacs.9b11515

(54) Chen, S.-M.; Xiong, J.; Zhang, Y.-Q.; Yuan, Q.; Wang, B.-W.; Gao, S. A soft phosphorus atom to “harden” an erbium(III) single-ion magnet. *Chem. Sci.* **2018**, *9*, 7540-7545. DOI: https://doi.org/10.1039/C8SC01626G

(55) Elkechai, A.; Mani, Y.; Boucekkine, A.; Ephritikhine, M. Density functional theory investigation of the redox properties of tricyclopentadienyl- and phospholyluranium(IV) chloride complexes. *Inorg. Chem.* **2012**, *51*, 6943-6952. DOI: https://doi.org/10.1021/ic300811m

(56) Greer, S. M.; Üngor, Ö.; Beattie, R. J.; Kiplinger, J. L.; Scott, B. L.; Stein, B. W.; Goodwin, C. A. P. Low-spin 1,1'-diphosphametallocenates of Chromium and Iron. *Chem. Commun.* **2020**, *57*, 595-598. DOI: https://doi.org/10.1039/D0CC06518H

(57) Gradoz, P.; Baudry, D.; Ephritikhine, M.; Lance, M.; Nierlich, M.; Vigner, J. Tetramethylphospholyluranium complexes and their pentamethylcyclopentadienyl analogues. *J. Organomet. Chem.* **1994**, *466*, 107-118. DOI: https://doi.org/10.1016/0022-328X(94)88035-2

(58) Izod, K.; Liddle, S. T.; Clegg, W. A convenient route to lanthanide triiodide THF solvates. Crystal structures of $LnI_3(THF)_4$ [Ln = Pr] and $LnI_3(THF)_{3.5}$ [Ln = Nd, Gd, Y]. *Inorg. Chem.* **2004**, *43*, 214-218. DOI: https://doi.org/10.1021/ic034851u

(59) Westerhausen, M.; Ossberger, M. W.; Mayer, P.; Piotrowski, H.; Nöth, H. Synthesis and Spectroscopic and Structural Investigations of the 2,3,4,5-Tetraethylarsolides

and -stibolides of the Alkali Metals Sodium, Potassium, Rubidium, and Cesium. *Organometallics* **2004**, *23*, 3417-3424. DOI: https://doi.org/10.1021/om049767g

(60) Greer, S. M.; Üngor, Ö.; Beattie, R. J.; Kiplinger, J. L.; Scott, B. L.; Stein, B. W.; Goodwin, C. A. P. Low-spin 1,1′-diphosphametallocenates of chromium and iron. *Chem. Commun.* **2021**, *57*, 595-598. DOI: https://doi.org/10.1039/D0CC06518H

(61) Meermann, C.; Ohno, K.; Törnroos, K. W.; Mashima, K.; Anwander, R. Rare-Earth Metal Bis (dimethylsilyl) amide Complexes Supported by Cyclooctatetraenyl Ligands. *Eur. J. Inorg. Chem.* **2009**, *2009*, 76-85. DOI: https://doi.org/10.1002/ejic.200800649

(62) Windorff, C. J.; Sperling, J. M.; Albrecht-Schönzart, T. E.; Bai, Z.; Evans, W. J.; Gaiser, A. N.; Gaunt, A. J.; Goodwin, C. A. P.; Hobart, D. E.; Huffman, Z. K.; Huh, D. N.; Klamm, B. E.; Poe, T. N.; Warzecha, E. A Single Small-Scale Plutonium Redox Reaction System Yields Three Crystallographically-Characterizable Organoplutonium Complexes. *Inorg. Chem.* **2020**, *59*, 13301-13314. DOI: https://doi.org/10.1021/acs.inorgchem.0c01671

(63) Meermann, C.; Ohno, K.; Törnroos, K. W.; Mashima, K.; Anwander, R. Rare-Earth Metal Bis(dimethylsilyl)amide Complexes Supported by Cyclooctatetraenyl Ligands. *Eur. J. Inorg. Chem.* **2008**, *2009*, 76-85. DOI: https://doi.org/10.1002/ejic.200800649

(64) Mashima, K.; Takaya, H. A new convenient synthesis of cyclooctatetraenyllanthanide complexes: X-ray crystal structure of CeI(C_8H_8)$(THF)_3$. *Tetrahedron Letters* **1989**, *30*, 3697-3700. DOI: https://doi.org/10.1016/S0040-4039(01)80486-X

(65) Mashima, K.; Nakayama, Y.; Nakamura, A.; Kanehisa, N.; Kai, Y.; Takaya, H. A new convenient preparation of monocyclooctatetraenyl-lanthanide complexes from metallic lanthanides and oxidants. *J. Organomet. Chem.* **1994**, *473*, 85-91. DOI: https://doi.org/10.1016/0022-328X(94)80108-8

(66) Bernbeck, M. G.; Orlova, A. P.; Hilgar, J. D.; Gembicky, M.; Ozerov, M.; Rinehart, J. D. Dipolar Coupling as a Mechanism for Fine Control of Magnetic States in ErCOT-

Alkyl Molecular Magnets. *J. Am. Chem. Soc.* **2024**, *146*, 7243-7256. DOI: https://doi.org/10.1021/jacs.3c10412

(67) Schwarz, N.; Krätschmer, F.; Suryadevara, N.; Schlittenhardt, S.; Ruben, M.; Roesky, P. W. Synthesis, Structural Characterization, and Magnetic Properties of Lanthanide Arsolyl Sandwich Complexes. *Inorg. Chem.* **2024**, *63*, 9520-9526. DOI: https://doi.org/10.1021/acs.inorgchem.3c03374

(68) Gordon, M. D.; Quin, L. D. Temperature dependence of ^{31}P NMR chemical shifts of some trivalent phosphorus compounds. *J. Magn. Reson.* **1976**, *22*, 149-153. DOI: https://doi.org/10.1016/0022-2364(76)90171-2

(69) Gorenstein, D. G. Chapter 1 - Phosphorus-31 Chemical Shifts: Principles and Empirical Observations. In *Phosphorous-31 NMR Principles and Applications*, Gorenstein, D. G. Ed.; Academic Press, 1984; pp 7-36.

(70) Shannon, R. D. Revised effective ionic radii and systematic studies of interatomic distances in halides and chalcogenides. *Acta Crystallogr. A* **1976**, *32*, 751-767. DOI: https://doi.org/10.1107/s0567739476001551

(71) Kilimann, U.; Schäfer, M.; Herbst-Irmer, R.; Edelmann, F. T. Cyclooctatetraenyl-komplexe der frühen übergangsmetalle und lanthanoide: III. Cyclooctatetraenyl-lanthanoidtriflate und -iodide: Neue ausgangsmaterialien für die organolanthanoid-chemie. *J. Organomet. Chem.* **1994**, *469*, C10-C14. DOI: https://doi.org/10.1016/0022-328X(94)80090-1

(72) Fedushkin, I. L.; Bochkarev, M. N.; Dechert, S.; Schumann, H. A Chemical Definition of the Effective Reducing Power of Thulium(II) Diiodide by Its Reactions with Cyclic Unsaturated Hydrocarbons. *Chem. Eur. J.* **2001**, *7*, 3558-3563. DOI: https://doi.org/10.1002/1521-3765(20010817)7:16<3558::AID-CHEM3558>3.0.CO;2-H

(73) Harriman, K. L. M.; Korobkov, I.; Murugesu, M. From a Piano Stool to a Sandwich: A Stepwise Route for Improving the Slow Magnetic Relaxation Properties of Thulium. *Organometallics* **2017**, *36*, 4515-4518. DOI: https://doi.org/10.1021/acs.organomet.7b00449

(74) Hilgar, J. D.; Bernbeck, M. G.; Flores, B. S.; Rinehart, J. D. Metal–ligand pair anisotropy in a series of mononuclear Er–COT complexes. *Chem. Sci.* **2018**, *9*, 7204-7209. DOI: https://doi.org/10.1039/C8SC01361F

(75) Hilgar, J. D.; Bernbeck, M. G.; Rinehart, J. D. Million-fold Relaxation Time Enhancement across a Series of Phosphino-Supported Erbium Single-Molecule Magnets. *J. Am. Chem. Soc.* **2019**, *141*, 1913-1917. DOI: https://doi.org/10.1021/jacs.8b13514

(76) Münzfeld, L.; Schoo, C.; Bestgen, S.; Moreno-Pineda, E.; Köppe, R.; Ruben, M.; Roesky, P. W. Synthesis, structures and magnetic properties of $[(\eta^9\text{-}C_9H_9)Ln(\eta^8\text{-}C_8H_8)]$ super sandwich complexes. *Nat. Commun.* **2019**, *10*, 3135. DOI: https://doi.org/10.1038/s41467-019-10976-6

(77) Tricoire, M.; Münzfeld, L.; Moutet, J.; Mahieu, N.; La Droitte, L.; Moreno-Pineda, E.; Gendron, F.; Hilgar, J. D.; Rinehart, J. D.; Ruben, M.; Le Guennic, B.; Cador, O.; Roesky, P. W.; Nocton, G. Size-Controlled Hapticity Switching in $[Ln(C_9H_9)(C_8H_8)]$ Sandwiches. *Chem. Eur. J.* **2021**, *27*, 13558-13567. DOI: https://doi.org/10.1002/chem.202101599

(78) Burton, N. C.; Cloke, F. G. N.; Hitchcock, P. B.; de Lemos, H. C.; Sameh, A. A. Scandium, yttrium, uranium, and thorium derivatives of the 1,4-bis(trimethylsilyl)cyclo-octatetraene dianion; the X-ray crystal structure of $[Sc_2(\eta\text{-}C_8H_6\{1,4\text{-}(SiMe_3)_2\})_2(\mu\text{-}Cl)_2(\mu\text{-thf})]$(thf = tetrahydrofuran). *J. Chem. Soc., Chem. Commun.* **1989**, 1462-1464. DOI: https://doi.org/10.1039/C39890001462

(79) Zhou, Z.; Greenough, J.; Wei, Z.; Petrukhina, M. A. The dinuclear scandium(III) cyclooctatetraenyl chloride complex di-μ-chlorido-bis[(η^8-cyclooctatetraene)(tetrahydrofuran-κ*O*)scandium(III)]. *Acta Crystallogr. C* **2017**, *73*, 420-423. DOI: https://doi.org/10.1107/S2053229617005678

(80) Sun, X.; Münzfeld, L.; Jin, D.; Hauser, A.; Roesky, P. W. Silole and germole complexes of lanthanum and cerium. *Chem. Commun.* **2022**, *58*, 7976-7979. DOI: https://doi.org/10.1039/D2CC02810G

(81) Cendrowski-Guillaume, S. M.; Le Gland, G.; Nierlich, M.; Ephritikhine, M. A comparison of analogous 4f- and 5f-element compounds: Syntheses and X-ray crystal structures of the mixed sandwich complexes [M(η-C_8H_8)(L){$OP(NMe_2)_3$}] (M = Nd or U; L = η-C_5Me_5 or η-C_4Me_4P). *Eur. J. Inorg. Chem.* **2003**, *2003*, 1388-1393. DOI: https://doi.org/10.1002/ejic.200390180

(82) Černá, M.; Seed, J. A.; Garrido-Fernandez, S.; Janicke, M. T.; Scott, B. L.; Whitehead, G. F. S.; Gaunt, A. J.; Goodwin, C. A. P. Isostructural σ-hydrocarbyl phospholide complexes of uranium, neptunium, and plutonium. *Chem. Commun.* **2022**, *58*, 13278-13281. DOI: https://doi.org/10.1039/D2CC04803E

(83) *Rigaku Oxford Diffraction, (2023), CrysAlisPro Software system, version 1.171.43, Rigaku Corporation, Wroclaw, Poland.*; Rigaku Oxford Diffraction: 2023.

(84) Dolomanov, O. V.; Bourhis, L. J.; Gildea, R. J.; Howard, J. A. K.; Puschmann, H. OLEX2: a complete structure solution, refinement and analysis program. *J. Appl. Crystallogr.* **2009**, *42*, 339-341. DOI: https://doi.org/10.1107/s0021889808042726

(85) Sheldrick, G. M. A short history of SHELX. *Acta Crystallogr. A* **2008**, *64*, 112-122. DOI: https://doi.org/10.1107/S0108767307043930

(86) Sheldrick, G. M. Crystal structure refinement with SHELXL. *Acta Crystallogr. C* **2015**, *71*, 3-8. DOI: https://doi.org/10.1107/S2053229614024218

(87) *Persistence of Vision Raytracer (Version 3.6)*; Persistence of Vision Pty. Ltd.: 2004. https://www.povray.org.

(88) *GNU Image Manipulation Program (GIMP) (Version 2.10.38)*; The GIMP Team: 2024. https://www.gimp.org.

(89) *Inkscape: Open Source Scalable Vector Graphics Editor. https://inkscape.org/.*

(90) Clegg, W.; Blake, A. J.; Cole, J. M.; Evans, J. S. O.; Main, P.; Parsons, S.; Watkin, D. J. *Crystal Structure Analysis*; Oxford University Press, 2009. DOI: http://doi.org/10.1093/acprof:oso/9780199219469.001.0001.

(91) de Lauzon, G.; Charrier, C.; Bonnard, H.; Mathey, F.; Fischer, J.; Mitschler, A. X-Ray crystal structure and Diels–Alder reactivity of the 3,4-dimethyl-2H-phosphole dimer. *J. Chem. Soc., Chem. Commun.* **1982**, 1272-1273. DOI: https://doi.org/10.1039/C39820001272

(92) de Lauzon, G.; Charrier, C.; Bonnard, H.; Mathey, F. Etude de la protonation des anions phospholyles. Obtention de dimeres de phospholes −2H. *Tetrahedron Letters* **1982**, *23*, 511-514. DOI: https://doi.org/10.1016/S0040-4039(00)86875-6

(93) Charrier, C.; Bonnard, H.; De Lauzon, G.; Mathey, F. Proton [1,5] shifts in P-unsubstituted 1*H*-phospholes. Synthesis and chemistry of 2*H*-phosphole dimers. *J. Am. Chem. Soc.* **1983**, *105*, 6871-6877. DOI: https://doi.org/10.1021/ja00361a022